



저작자표시-비영리-변경금지 2.0 대한민국

이용자는 아래의 조건을 따르는 경우에 한하여 자유롭게

- 이 저작물을 복제, 배포, 전송, 전시, 공연 및 방송할 수 있습니다.

다음과 같은 조건을 따라야 합니다:



저작자표시. 귀하는 원저작자를 표시하여야 합니다.



비영리. 귀하는 이 저작물을 영리 목적으로 이용할 수 없습니다.



변경금지. 귀하는 이 저작물을 개작, 변형 또는 가공할 수 없습니다.

- 귀하는, 이 저작물의 재이용이나 배포의 경우, 이 저작물에 적용된 이용허락조건을 명확하게 나타내어야 합니다.
- 저작권자로부터 별도의 허가를 받으면 이러한 조건들은 적용되지 않습니다.

저작권법에 따른 이용자의 권리는 위의 내용에 의하여 영향을 받지 않습니다.

이것은 [이용허락규약\(Legal Code\)](#)을 이해하기 쉽게 요약한 것입니다.

[Disclaimer](#)

碩士學位論文

Meniscus Generation Methodologies of Electrostatic Inkjet for Printed Electronics

濟州大學校 大學院

메카트로닉스공학과

무하마드 아시프

2009 年 7月



碩士學位論文

Meniscus Generation Methodologies of Electrostatic Inkjet for Printed Electronics

濟州大學校 大學院

메카트로닉스공학과

무하마드 아시프

2009 年 7月

Meniscus Generation Methodologies of Electrostatic Inkjet for Printed Electronics

指導教授 崔 劉 賢

무하마드 아시프

이 論文을 工學 碩士學位 論文으로 提出함

2009年 7月

무하마드 아시프의 工學 碩士學位 論文을 認准함

審査委員長 _____ ⑩

委 員 _____ ⑩

委 員 _____ ⑩

濟州大學校 大學院

Meniscus Generation Methodologies of Electrostatic Inkjet for Printed Electronics

Muhammad Asif Ali Rehmani

(Supervised by professor Kyung-Hyun Choi, Jeju National University
and co-supervised by Dong-Soo Kim, KIMM)

A thesis submitted in partial fulfillment of the requirement for the degree of Master of
Science

2009 . 7.

This thesis has been examined and approved.

Thesis Committee Chair, Chul-Ung Kang, Prof. of Mechatronics Engineering

Thesis director, Kyung-Hyun Choi, Prof. of Mechatronics Engineering

Thesis Committee Member, Yang-Hoi Doh, Prof. of Electronics Engineering

Department of Mechatronics Engineering
GRADUATE SCHOOL
JEJU NATIONAL UNIVERSITY



Dedicated to

My Parents, Family and Teachers

ACKNOWLEDGEMENTS

I would like to extend my sincere and humble gratitude to almighty Allah Almighty, Who guided me in darkness, helped me in difficulties and provided me with courage, ability and honor to come this far and make contribution in sacred cause of learning and serving.

This dissertation could not have been written without the guidance of Prof Choi, Kyung Hyun who not only served as my supervisor but also encouraged and challenged me throughout my postgraduate studies. Prof. Choi provided me favoring research environment and vision to carry out my research. He took care of all the stumbling blocks which came by during my studies either they are in studies, related to finance or they are related to my family. I would also like to thank his wife who's affectionate support to my mother, wife and kids were immeasurable. I would like to thank my co-supervisor Prof. Kim, Prof. Doh and Prof. Kang who guided me through the dissertation process, never accepting less than my best efforts.

I am extremely grateful to Dr. Umer Zeeshan Ijaz who not only introduced me to my supervisor for postgraduate studies but also paved my path in attaining the postgraduate studies. He was instrumental in guiding me to start my higher studies and helped me in settling down in Jeju.

I have been fortunate enough to have had the support of so many people in the research group without them this thesis would not have been possible – Khalid Rahman, Ahsan Rahman, Thanh, Adnan Ali, Saleem Khan, Kim Chang Jong, Ko Jeong-beom, Yang Bong Soo, Dang Hyun Hoo and Tran Trung Thanh. I am also thankful to the wonderful friends Nauman & his family, Ahmer & his, Shafqat-ur-Rehman, Jasim & his family, Rakib & his family, Iskander and Afzaal who shared my high and lows of postgraduate studies.

I am deeply indebted to my parents who have been extremely understanding and supportive of my studies. Especially my father who provided me motivation and supported me financially to take care of my family during my postgraduate studies. I am also grateful to my mother who accompanied me during my postgraduate studies and shared the responsibilities of taken care of children and day-to-day matters. I would like to pay my heartiest gratitude to my wife Sobia who not only supported me throughout my postgraduate studies but also shared the responsibilities for taking care of my children when I was busy in my research. Without her support my accomplishment would have been undermined. I feel sorry for my daughter Alisha and my son Hamza who were neglected during the course of my studies. I hope I will make up for the time they spent without me in future. I would also like to thank my brother Wasif, my sister Aisha, my

in-laws and my extended family who encouraged me throughout my studies and provided me the necessary moral support.

In the end I would like to honor the lovable and respectful Korean people who supported me when I was in trouble despite of language barrier. They are the wonderful nation and deserve more than mentioned here. I thank them all.



CONTENTS

1	INTRODUCTION	3
1.1	Background -----	3
1.2	Motivation -----	4
1.3	Thesis Overview -----	4
2	PRINTED ELECTRONICS	7
2.1	Introduction -----	7
2.2	Future Trend and Forecast -----	9
2.3	Key Printed Technologies -----	12
2.4	Inkjet Printing -----	13
2.4.1	<i>Thermal Inkjet</i> -----	13
2.4.2	<i>Piezoelectric Inkjet</i> -----	14
2.4.2.1	Squeeze Mode PIJ -----	15
2.4.2.2	Bend Mode PIJ -----	15
2.4.2.3	Push Mode PIJ -----	16
2.4.2.4	Shear mode actuator -----	16
2.4.3	<i>Electrostatic Inkjet</i> -----	17
2.4.4	<i>Comparison Drop-on-Demand Technology</i> -----	18
2.5	Applications -----	18
3	ELECTROSTATIC PRINTING AND MENISCUS GENERATION	20
3.1	Related Work -----	20
3.2	Advantages of Electrostatic Inkjet Printing in PE -----	22
3.3	Meniscus Generation and its Role -----	22
3.4	Printing and Meniscus Generation Strategies -----	23
3.4.1	<i>Constant flow regulated Inkjet Printing</i> -----	24
3.4.1.1	Problem Definition -----	25
3.4.1.1.1	Varying Channel Width Geometry with Non-Tapered Supply Channel -----	25
3.4.1.1.2	Varying Channel Width Geometry with Tapered Supply Channel -----	26
3.4.1.1.3	Electrokinetic assisted constant channel geometry -----	26
3.4.1.2	Electrokinetic Theoretical background -----	27
3.4.1.3	Numerical Estimation Parameters -----	28
3.4.2	<i>Piezoelectric Hybrid Inkjet System</i> -----	29
3.4.2.1	Problem Definition -----	30
3.4.2.2	Theoretical Background -----	31
3.4.2.2.1	Piezo-electric Actuation -----	31
3.4.2.2.2	Electrostatic Actuation -----	32
3.4.2.3	Numerical Estimation Parameters and Approach -----	36
4	RESULTS AND INTERPRETATION	37
4.1	Varying Channel Width Geometry with Non-Tapered Supply Channel -----	37
4.2	Varying Channel Width Geometry with Tapered Supply Channel -----	39
4.3	Electrokinetic assisted constant channel geometry -----	41
4.4	Piezo-Electrostatic Hybrid Inkjet Head -----	46
4.4.1	<i>Numerical Estimation of piezoelectric pressure generation</i> -----	46
4.4.2	<i>Numerical Estimation of Meniscus generation</i> -----	50
4.4.3	<i>EHD numerical estimation of pre-developed meniscus droplet generation</i> -----	53
4.4.4	<i>EHD numerical estimation of without meniscus developed droplet generation</i> -----	55

5 SUMMARY AND CONCLUSION	59
5.1 Conclusion for constant flowrate -----	59
5.2 Conclusion for Hybrid Piezo-Assisted -----	60
References	61



LIST OF FIGURES

Figure 2.1	Printed Electronics Vs Conventional Electronics -----	7
	--	
Figure 2.2	Conventional Integrated Chip Manufacturing Process Vs Inkjet Process -----	8
	-	
Figure 2.3	Forecasted market for flexible and non-flexible printed electronics -----	9
	-	
Figure 2.4	Forecasted market by components for printed electronics -----	10
	-	
Figure 2.5	Contribution Towards Printed Electronics by Territory -----	11
	-	
Figure 2.6	Contribution towards printed electronics in East Asia by Region -----	11
	--	
Figure 2.7	Classification of inkjet Technology -----	13
	-	
Figure 2.8	Thermal Inkjet: Principle of Operation -----	14
	-	
Figure 2.9	Squeeze Mode: Principle of Operation -----	15
	--	
Figure 2.10	Bend Mode: Principle of Operation -----	15
	-	
Figure 2.11	Push Mode Inkjet: Principle of Operation -----	16
	-	
Figure 2.12	Shear Mode Inkjet: Principle of Operation -----	16
	--	
Figure 2.13	Electrostatic Inkjet: Principle of Operation -----	17
	-	
Figure 3.1	Forces acting against the ejection of droplet during piezoelectric actuation -----	23
	--	
Figure 3.2	Varying Channel Width Geometry with Non-Tapered Supply Channel-----	26
	-	
Figure 3.3	Varying Channel Width Geometry with Tapered Supply Channel-----	26
	--	
Figure 3.4	Electrokinetic assisted constant channel geometry-----	27
	-	
Figure 3.5	Cross-sectional layout of the proposed device -----	30
	--	
Figure 3.6	Forces acting on the sessile drop under electrostatic forces -----	33
	--	
Figure 3.7	Numerical Estimation Step for Piezo-Electrostatic hybrid head -----	36
	-	
Figure 4.1	Flow simulation for the varying channel width geometry of secondary nozzle with non-tapered primary supply channel. Flowrate across the secondary nozzle for 25 μ l/hr primary channel flowrate -----	37
	--	
Figure 4.2	Flow simulation for the varying channel width geometry of secondary nozzle with non-tapered primary supply channel. Flowrate across the secondary nozzle for 175 μ l/hr primary channel flowrate -----	38

Figure 4.3	Flow simulation for the varying channel width geometry of secondary nozzle with non-tapered primary supply channel. Flowrate across the secondary nozzle for 200 μ l/hr primary channel flowrate -----	38
Figure 4.4	Flow simulation for the varying channel width geometry of secondary nozzle with tapered primary supply channel. Flowrate across the secondary nozzle for 25 μ l/hr primary channel flowrate -----	39
Figure 4.5	Flow simulation for the varying channel width geometry of secondary nozzle with tapered primary supply channel. Flowrate across the secondary nozzle for 175 μ l/hr primary channel flowrate -----	40
Figure 4.6	Flow simulation for the varying channel width geometry of secondary nozzle with tapered primary supply channel. Flowrate across the secondary nozzle for 200 μ l/hr primary channel flowrate -----	40
Figure 4.7	Surface gradient of the electric field and streamlines for the electrokinetic flow ----	41
Figure 4.8	Coupled electrostatic and flow simulation for the electrokinetic driven flow from the secondary outlet of the nozzles. Surface velocity profile and electrostatic force direction for the 25 μ l/hr inlet flowrate -----	42
Figure 4.9	Electrokinetic force on different subdomain of the proposed electrokinetic fluidic channel -----	42
Figure 4.10	Flow simulation for the electrokinetic fluidic pumping channel. Flowrate across the secondary nozzles for 25 μ l/hr primary channel flowrate -----	43
Figure 4.11	Flow simulation for the electrokinetic fluidic pumping channel. Flowrate across the secondary nozzle for 175 μ l/hr primary channel flowrate -----	43
Figure 4.12	Flow simulation for the electrokinetic fluidic pumping channel. Flowrate across the secondary nozzles for 200 μ l/hr primary channel flowrate -----	44
Figure 4.13	Varying voltage at the secondary outlets to achieve the constant flowrate -----	45
Figure 4.14	Voltage function in domain for piezoelectric numerical estimation -----	46
Figure 4.15	Numerical estimation parameters for piezoelectric simulation -----	47
Figure 4.16	Pressure generated in the ink chamber at different frequencies w.r.t. applied voltage	48
Figure 4.17	Numerical estimation parameters for Two—Phase flow meniscus generation simulation -----	50
Figure 4.18	Meniscus generation by means of piezo generated pressure in time domain at every 3 μ s -----	51
Figure 4.19	Meniscus height in time domain w.r.t. applied pressure through piezoelectric actuator -----	52
Figure 4.20	Numerical parameters for Meniscus Generated EHD Simulation -----	53
Figure 4.21	Droplet generation in time domain for pre-developed meniscus through piezoelectric actuator -----	54

Figure 4.22	-- Numerical parameters for without Meniscus Generated EHD Simulation -----	55
Figure 4.23	-- Droplet Generation process in Electrode Protruded conventional Electrostatic Inkjet Head -----	56
Figure 4.24	-- Comparison of Droplet Generation of Hybrid Electro-Piezoelectric and Electrostatic Inkjet -----	58
	--	



LIST OF TABLES

Table 2.1	Key Contact and Contact Less Printing Technologies -----	12
Table 2.2	Comparison of Piezoelectric and Thermal Inkjet Printing -----	18
Table 3.1	Numerical simulation parameters of the electrokinetic fluidic channels and flowrate for all the microfluidic channel geometries -----	28
Table 3.2	Numerical simulation parameters for Piezo-Electrostatic hybrid head -----	36
Table 4.1	Numerical simulation geometric parameters of the nozzle opening of each geometry -----	44
Table 4.2	Response of PZT-5H -----	49
Table 4.3	Boundary Conditions for Meniscus Generated EHD Simulation -----	53
Table 4.4	Boundary Conditions for conventional Electrostatic Inkjet Simulation -----	55



NOMENCLATURES

α	Polarizability of the atom or molecule
ϵ_0	Permittivity of the free space
ϵ	Relative electrical permittivity of the material
ρ	Density of the fluid
$\rho^{(e)}$	Total electric charge density per unit volume
φ	Electric potential/ Voltage
η	Kinematic viscosity
μ	Dynamic viscosity
γ	Surface tension
P	Polarization vector
Q	Magnitude of charge separated to produce dipole
R_n	Capillary radius
A_n	Cross-sectional area of nozzle
L_n	Characteristic length of the nozzle
V	volume
u	Velocity of the fluid
t	Time
P	Pressure
g	Acceleration due to gravity
T^m	Mechanical stresses of the fluid
T^e	Electric stresses of the fluid
q	Charge density
E	Electric field

요약문

전도성 라인을 프린팅하기 위한 정전기력 프린팅 방식의 성공적인 연구결과 발표에도 불구하고 인쇄 전자 부품 제조를 위한 기술은 지금까지 상용화가 이루어지지 않은 실정이다. 정전기력 잉크젯 시스템의 노즐에서 액적의 토출을 위한 높은 전압의 요구가 상용화의 걸림돌이 되고 있다. 기존 문헌에서 분석된 정전기력 잉크젯 연구는 금속 모세관을 통하여 잉크를 충전하거나 니들 내부의 충전 전극을 이용하는 실험적인 내용이 대부분이다. 상대적으로 작은 크기의 마이크로 채널 때문에 충전 전극에 의해 생성된 정전기력의 대부분이 흡수되거나 소멸시키는 큰 표면 점성력을 갖는다.

본 논문에서는 충전 전극이 노즐에서 액적을 토출하기 위한 정전기력을 발생시킬 때 잉크 챔버 내부의 점성력의 영향을 제거하거나 감소시키기 위하여 동전기(Electro Kinetic) 기반의 잉크 공급 메커니즘을 제안하고자 한다. 또한, 압전 구동을 통하여 사전 형성된 메니스커스의 도움으로 정전기력 잉크젯 헤드의 에너지 요구치를 줄이는 압전과 정전기기반의 새로운 하이브리드 장치를 제안하고자 한다. 제안된 개념에서는 메니스커스는 전극 끝단에 형성이 되며, 전극의 끝단에 높은 변화도(gradient)의 정전기 전위가 생성된다. 잉크가 노즐 외부에 있기 때문에 좁은 채널로 인한 노즐 점성력은 상당히 감소한다. 잉크는 이미 가속되어 토출 직전의 끝단에 전달이 되기 때문에 잉크를 가속하는데 필요한 동적 압력도 역시 감소한다.

본 개념은 정전기력 잉크젯 토출을 위한 새로운 방식일 뿐만 아니라 토출을 제한하는 힘들 줄이는 시도를 통하여 정전기력 잉크젯 공정을 최적화를 구현할 수 있는 기회를 부여한다. 또한, 본 논문에서는 액적의 토출에 대하여 사전 형성된 메니스커스 방식과 정전기력만으로 형성되는 메니스커스 방식 및 콘젯 방식에 의한 토출 액적의 크기를 비교 분석 하였으며, 제안된 새로운 개념은 토출 액적의 크기를 상당히 줄였으며 액적 생성을 위한 정전기 전위 또한 줄어 들었음을 증명하였다.

ABSTRACT

Even after the successful demonstration of the electrostatic printing method for generating the printed conductive lines the method was not commercialized until now for printed electronic fabrication. This is due to the application of high voltage for the ejection of the droplet being reported and high throughput. Most of the electrostatic inkjet setup found in the literature was studied experimentally by charging the ink through metal capillary or using a charging wire inside the needle. Due to the relatively small dimension of the micro-channel it poses immense surface viscous force that most of the electrostatic force exerted by the charging electrode is absorbed or disseminated due to the viscous forces.

In the work presented in this thesis an electrokinetic ink pumping mechanism is suggested to overcome or subsidize the effect of viscous forces inside the ink chamber when the charging electrode exerts the electrostatic forces to eject the droplet from the nozzle. In addition to the micro-pumping mechanism a novel hybrid piezoelectric and electrostatic device is proposed for reducing energy requirement of the electrostatic inkjet head with the help of pre-developed meniscus through piezoelectric actuation. In the proposed concept the meniscus is generated at the tip of the electrode and the electrostatic potential is applied which has its highest gradient at the electrode apex. Since the liquid is already outside the nozzle therefore the nozzle viscous forces due to the narrow channel is subsidized considerably. It is also pertinent to mention here that the liquid is already accelerated and is transported at the tip of the ejection election therefore the dynamic pressure required to accelerate the liquid is also subsidized.

This concept is not only the first of its kind to be presented for the electrostatic inkjet ejection but it also enables the current researchers to optimized the electrostatic inkjet printing by reducing the forces which acts against the generation of the drop. Furthermore the proposed concept also provides the comparison of droplet size for pre-developed meniscus and electrostatically developed meniscus and conejet for the ejection of the drop. It was demonstrated that the novel concept proposed in this study reduces the size of the droplet considerably and also reduces the electrostatic potential for droplet generation.

1 INTRODUCTION

1.1 BACKGROUND

In the last decade there has been tremendous focus on producing cheaper technology which can replace micron level low throughput MEMs manufacturing with the focus of printing on the flexible substrate. Thermal or piezo driven inkjet technology is widely in use for physical document archiving and fabrication of printed electronic devices. Both of these technologies have been matured and are being in use for the last three or four decades (Elmqvist 1951, Sweet 1965 & 1971, Buehner et al., 1968-1977). Albeit the drop-on-demand droplet can be achieved through these technologies but these are also confronted by the challenges in the printed electronic industry. For instance thermal inkjet which works on the principle of forming a minute bubble in the ink chamber by heating element and displacing enough volume in the ink chamber so that the droplet can be ejected through the nozzle outlet has two major drawbacks. First, the thermal sensitive liquid in the ink chamber cannot be used as a working fluid and secondly it is difficult to achieve smaller droplet size than the nozzle outlet diameter. These drawbacks put the limitation on the usage of thermal inkjet printhead to be utilized for fabricating electronic devices since the ink characteristics changes due to heating especially in case of biomedical devices. Whereas in case of piezoelectric inkjet printhead some of the issues pertaining to thermal inkjet such as the use of thermal sensitive ink and higher print frequencies can be addressed but generation of droplet size smaller than the diameter of nozzle remains in question. Moreover, the high fluidic channel resistance offers physical challenges in overcoming the ink chamber pressure and generating the necessary pressure for droplet size smaller diameter through piezoelectric printheads.

Improvement in the produced image quality, printing speed, printing resolution and accuracy is under constant demand. In order to confront these challenges electrostatic inkjet printing seems to be the promising technology in addressing the bottlenecks in the printed electronic industry for fabricating devices at higher throughput and resolution.

Even though the thermal and piezo driven inkjet technology offers one of the solution to produce cheaper fabrication process for producing high throughput printing of micro drop with appreciable control over the placement of drop but the drop size has the limitations. Firstly the drop size smaller than the nozzle orifice size is difficult to achieve, secondly droplet generation

through outlet orifice smaller than $30\mu\text{m}$ is difficult to achieve. Moreover in case of thermal inkjet process the thermal dissipation of electric heater in the ink chamber to form the bubble responsible for droplet ejection put limitation on the usage of ink. For the same reason in many bio applications thermal inkjet printing doesn't seem to be applicable.

1.2 MOTIVATION

The Electrostatic inkjet provides the solution to the aforementioned challenges but the device itself is difficult to fabricate and offers research challenges. Due to its complex integration in the existing printing technology and drive for achieving smaller droplet size; this field offers exciting opportunity. Stable meniscus generation ensures uniform printing and provides the ink at the fluid ejection zone such that the driving energy for the droplet generation can be reduced. The proposed work in this thesis explores the possible solution by proposing the method of providing the necessary flowrate and meniscus generation strategies to be able to utilize the electrostatic potential in a pragmatic manner for achieving a smaller droplet size.

1.3 THESIS OVERVIEW

In this thesis two issues pertaining to the electrostatic inkjet printhead. First the ink supply mechanism has been discussed for providing the constant flowrate across the horizontal fluidic channel. In this approach a set of three nozzles which are connected to a main horizontal supply are designed with three distinct approaches for achieving the constant flow rate across the fluidic channel. It was found that it is possible to achieve constant flowrate through a main horizontal channel under the external pumping but the scalability to a wider array of nozzle is difficult to achieve and for the same reason the horizontal channel under the pressurized external pumping is not much in practice for designing an existing piezo-actuated printhead. Whereas there are numerous examples available for the static horizontal supply under static pressure. It is also shown in the work presented in this thesis that for a conductive liquid it is possible to achieve the constant flowrate across the fluidic channel and electrokinetic pumping can be achieved for the electrostatic printhead for horizontal supply under the influence of external pumping for a limited number of nozzles.

The second section of the thesis presents the potential concept of the hybrid piezo and electrostatic printhead. Efforts has been made to provide recommendations through a numerical study of such a printhead and outlines the advantages which can be harvested by using both the actuating force (piezoelectric generated pulse pressure and electrostatic force) in tandem for achieving the smaller droplet size. This case study has been done by segregating the forces in time domain which acts on such a system. For instance for the first few microseconds the piezoelectric force is used to generate the meniscus. After the meniscus has been generated by the pressure force being induced by the piezoelectric actuation the electrostatic pulse is being given to the ink charging electrode to produce the droplet. It is also pertinent to mention here that the electrode is placed such that apex of the meniscus has the strongest electric field so that the thin conejet can be achieved for smaller droplet size. In the end a comparison is also provided for the droplet ejected by means of electrostatic force with meniscus formation due to the piezoelectric force and without the meniscus. It was found that the droplet size and electrostatic voltage potential can be reduced considerably in a hybrid piezoelectric and electrostatic printhead.

Futhermore the thesis provides the overview of printed electronics with reference to flexible printing and its importance by keeping in view the market investment for producing printed electronic devices. The role of electrostatic printing is also highlighted for potential benefit that can be achieved through electrostatic inkjet printing.

The forth coming compilation of the dissertation is as follows

Chapter 2 provides the overview of the emerging printing electronics market with the share of the inkjet printing technology in that market and details the existing printing technology. Furthermore, it outlines the role of inkjet printing in printed electronics.

Chapter 3 outlines the proposed method for generating the meniscus and supplying ink at the orifice outlet with the theoretical background of each of the proposed method.

Chapter 4 discusses the result being obtained through the simulation of the proposed method and highlights the benefits of the proposed method of generating the meniscus and its efficacy in obtaining the smaller droplet size through electrostatic inkjet printing.

Chapter 5 presents the summary of the dissertation, draws conclusion to the research and sheds light on possible enhancements in the proposed work.



2 PRINTED ELECTRONICS

2.1 INTRODUCTION

Printed electronics is a set of printing methods used to create electrically functional devices. Paper has been often proposed to be used as substrate but due the rough surface and high humidity absorption other materials such as plastic, ceramics and silicon has been applied more widely. Several printing processes have been piloted and printing preferably utilizes common printing equipment in the graphics arts industry, such as screen printing, flexography, gravure, offset lithography and inkjet. Instead of printing graphic arts inks, families of electrically functional electronic or optical inks are used to print active or passive devices, such as thin film transistors or resistors. Printed electronics is expected to facilitate widespread and very low-cost, low-performance electronics useful for applications not typically associated with conventional high performance (i.e., silicon-based) electronics, such as flexible displays, smart labels, decorative and animated posters, and active clothing.

The term printed electronics is often used in association with organic electronics or plastic electronics, where one or more functional inks are composed of carbon-based compounds. While these other terms refer to the material system, the process used to deposit them can be either solution-based, vacuum-based, or some other method. Printed electronics, in contrast, specifies the process, and can utilize any solution-based material, including organic semiconductors, inorganic semiconductors, metallic conductors, nanoparticles, nanotubes, etc. Electronic applications with high switching frequencies and high integration density (so-called "high-end electronics") will be dominated for a foreseeable future by conventional electronics, which in turn needs high investment and fabrication costs. In contrast, printed electronics as a complementary technology targets at the establishment of a "low-cost electronics" for application fields, where the high performance of conventional electronics is not necessary as shown in fig. 2.1.

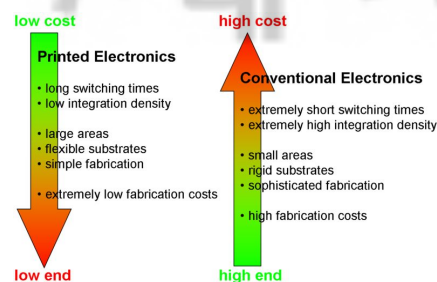


Figure 2.1. Printed Electronics Vs Conventional Electronics

Inkjet printing is one of the methods of generating microdrop as a substitute process for conventional manufacturing of electronic integrated chip as shown in fig. 2.2. There are numerous application of such a microdrop generated through inkjet process and more specifically drop-on-demand inkjet process. It will be of foremost importance that the drop-on-demand inkjet printer provides high printing speed with higher printing resolution. Since electrostatic printing can address both the in-demand issues for the printing therefore it has numerous application in printed electronic devices such as RFID, flexible display, solar cell, sensors, batteries etc (Ishida et al., 2008). Moreover contact-less drop on demand printing scheme is very appealing technique to fabricate different electronics and electrical patterns as this technique has advantages over conventional photolithography technique in source dissipation and energy level (Heinzl and Hertz 1985, Le 1998).

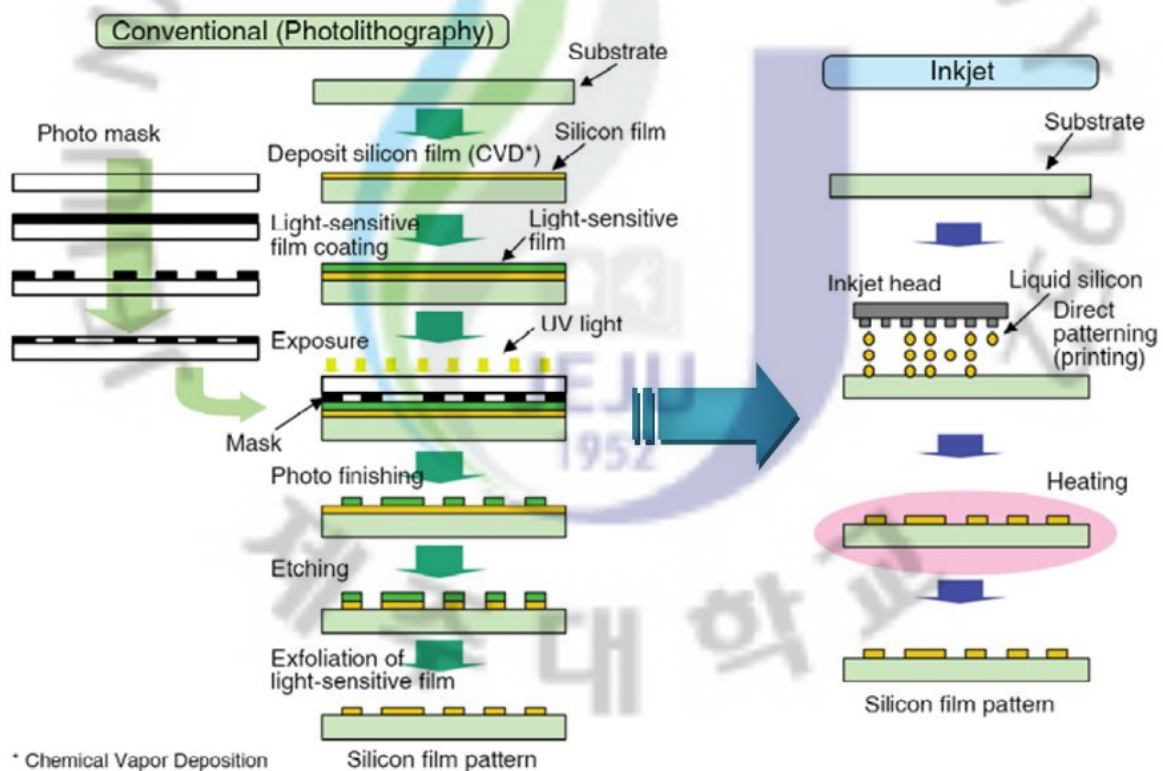


Figure 2.2. Conventional Integrated Chip Manufacturing Process Vs Inkjet Process

2.2 FUTURE TREND AND FORECAST

The present technology trend is gathering momentum towards the application of the flexible devices since these device can easily adhere the shape of the surface they are being deployed. This single advantage is so enthralling as the application of the printed functional devices can be seamlessly employed without the significant changes in the existing infrastructure and its economic viability in terms of return/earning on investments. For the same reason the continuously evolving and maturing flexible printed electronic industry shows a steep increase in the forecasted printed electronic industry share as being depicted in the fig. 2.3.

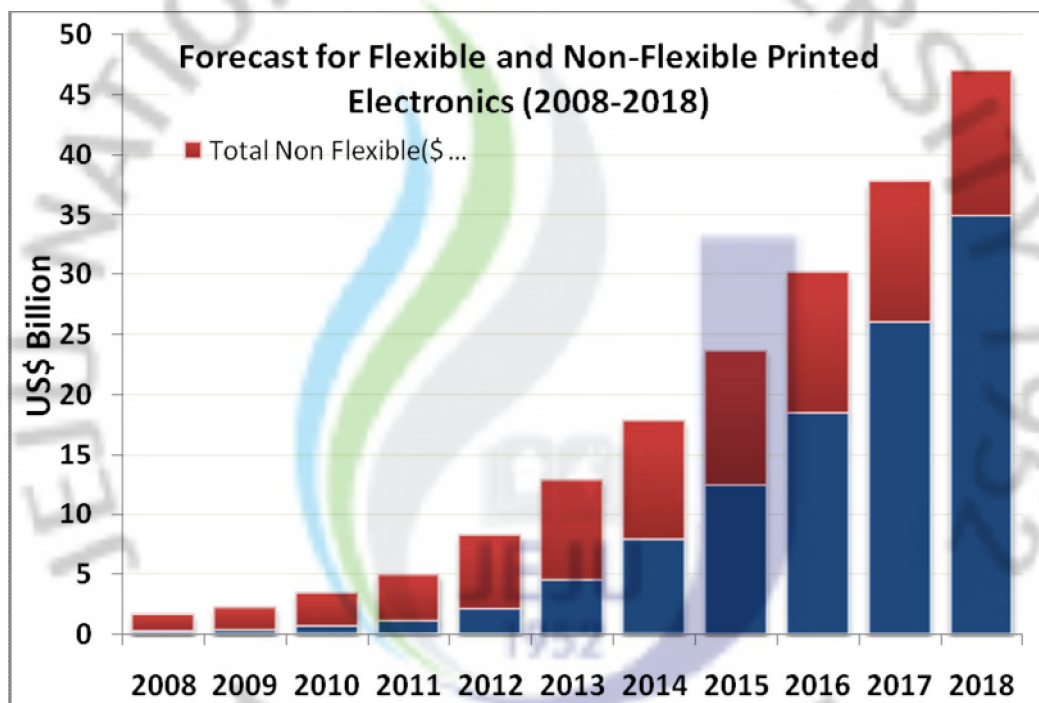


Figure 2.3. Forecasted market for flexible and non-flexible printed electronics (Source: IDtechEx)

Consumer market will be one of the main market for printed electronic applications. OLED displays, OLED lighting, Photovoltaic and logic memory will be burgeoning market for the printed electronic industry. Fig 2.4 shows the forecasted component wise distribution for printed electronics.

Market Forecast for Printed Electronics Components by 2028

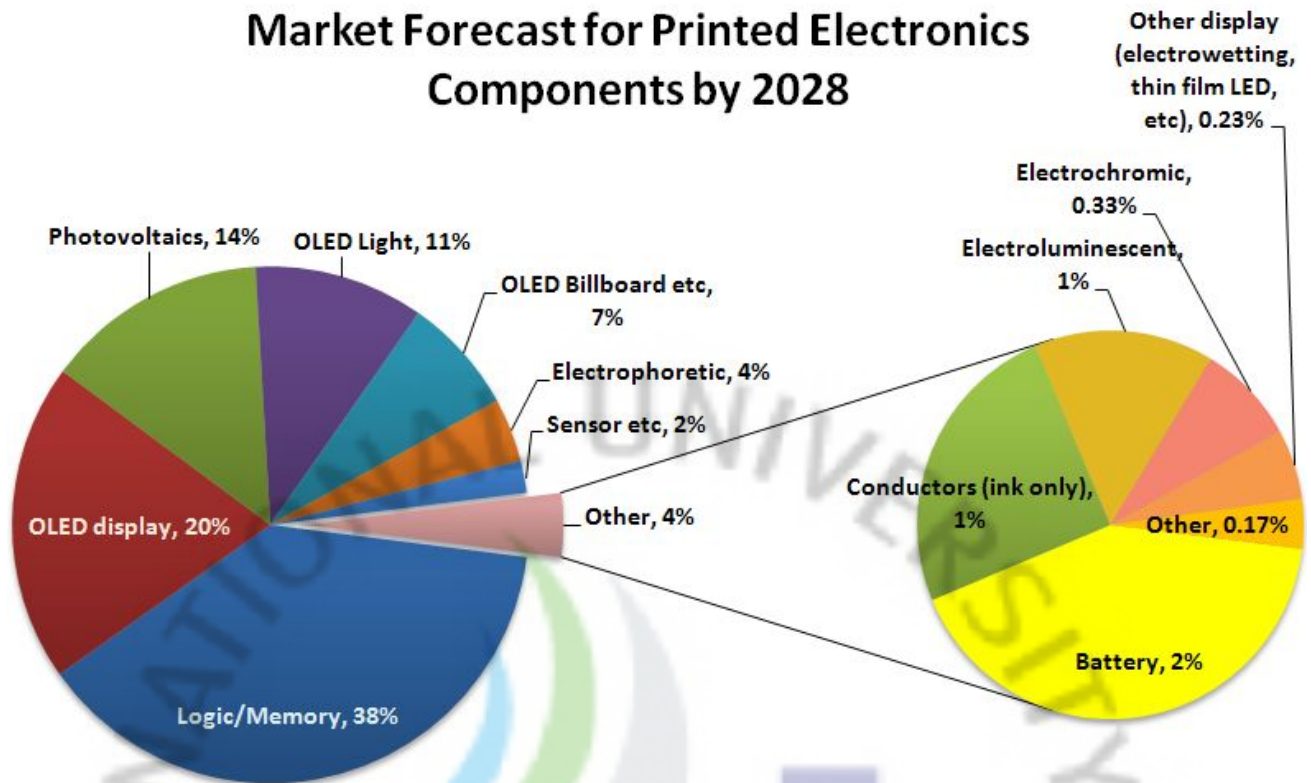


Figure 2.4 . Forecasted market by components for printed electronics (Source: IDtechEx)

Inkjet printing proves to be a promising fabrication technology for printed electronics devices. Issues pertaining to the printing resolution and replacing the expensive Micro-Electro-Mechanical (MEMs) lithography fabrication techniques cannot be justified for some of the present electronic devices to be scaled for the consumer markets. It is a daunting task for the inkjet technology to replace the traditional MEMs process for the fabrication of cheap electronic devices by improving the print resolution. United States followed by Asia Pacific and Europe respectively will be the most contributing nations to the printed electronic industry. It is also envisaged that the future fabrication trend of printed electronics will lean towards the technology which can produce the cheaper printing technology. Fig 2.5 shows the forecasted contribution towards the printed electronic by Territory.

Contribution Towards Printed Electronics in by Territory in \$ billion

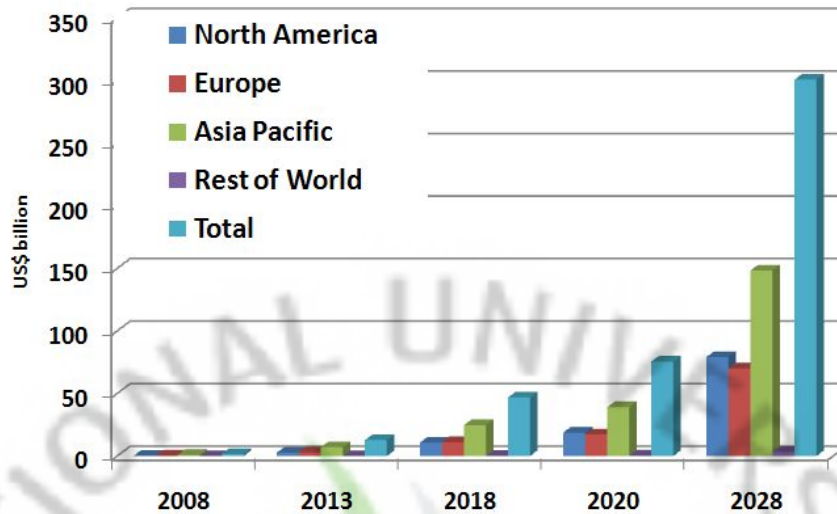


Figure 2.5. Contribution Towards Printed Electronics by Territory (Source: IDtechEx)

South Korea will be the major contributor in Asia for the printed industry due to its huge market share in the display and consumer market. This also provides the importance of printed electronics in this region. Fig. 2.6 shows the expected market share of East Asia by region.

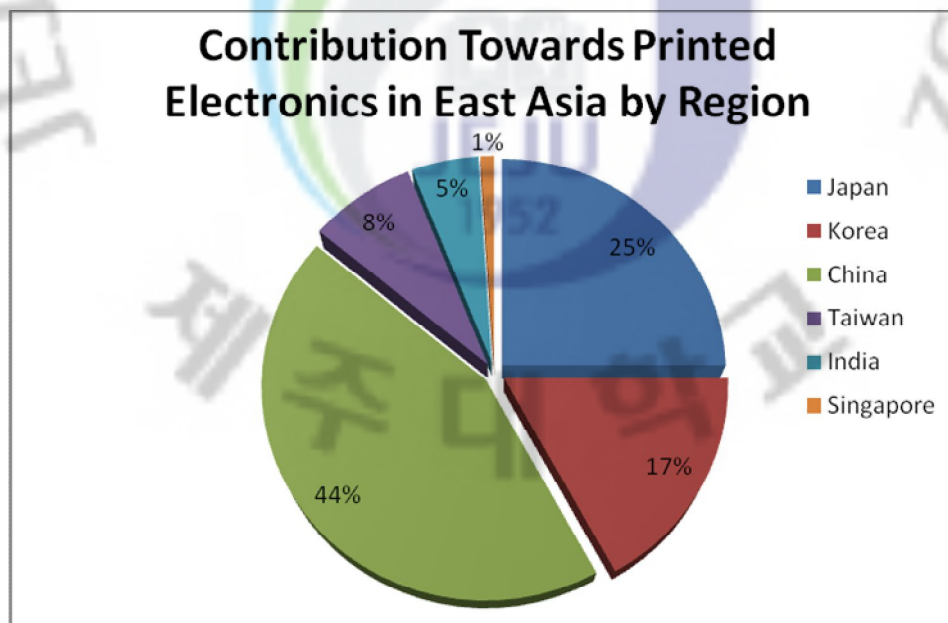


Figure 2.6. Contribution towards printed electronics in East Asia by Region (Source: IDtechEx)

2.3 KEY PRINTED TECHNOLOGIES

Primarily the key printed technologies can be divided into contact printing and the contact less printing method. Contact less printing mainly comes into the inkjet technology. Table 2.1 below shows the key printing technologies under the contact and contact less printing.

Table 2.1. Key Contact and Contact Less Printing Technologies

Contact Printing Technologies	Contact Less Printing Technologies
Screen Printing	Aerosol Inkjet Printing
Offset Printing	Thermal Inkjet Printing
Flexography Printing	Piezoelectric Inkjet Printing
Gravure Printing	Electrostatic Inkjet Printing
Pad Printing	Acoustic Inkjet Printing

Contact printing is widely in use in paper industry and print media. Advantage of this printing method is the high throughput with accuracies upto 50 μ m (Hughes and Ernster 2003). Whereas the gravure printing can reach higher resolution and high aspect ratio. Almost all of contact printing method utilizes the roll-to-roll technology to transfer the base pattern on the substrate. Whereas the registration control in case of tight tolerances can be challenging since the printing pressure is high with high web velocity and elastic nature of the flexible substrate makes it even more difficult. However the resulting product is cheaper than contact less printing method due to the high printing speed.

Inkjet printing has certain advantage in printed electronic application. Not only it is a contact less printing method but also a additive fabrication process which involves the pattern printing to be in a discrete or continuous manner depending upon the selection of the inkjet process. Moreover the emerging electrostatic printing can yield to high resolution of printer than the former processes.

2.4 INKJET PRINTING

Contactless inkjet printing is classified into two categories; continuous and drop-on-demand. Continuous inkjet printing is suitable for similar material deposition on the substrate and relatively low resolution printing. Since the deposition force is relatively higher and yield higher deposition velocity which is prone to offer more spreading on the substrate. Whereas the printing speed is fast as compared to the drop-on-demand process and is suitable for high printing throughput. However the equipment cost is high as compared with the on-demand inkjet printing setup.

Drop-on-demand inkjet printing provide more flexibility in terms of the ink deposition on the substrate and provide higher accuracy than the continuous printing. Various printing technologies under the

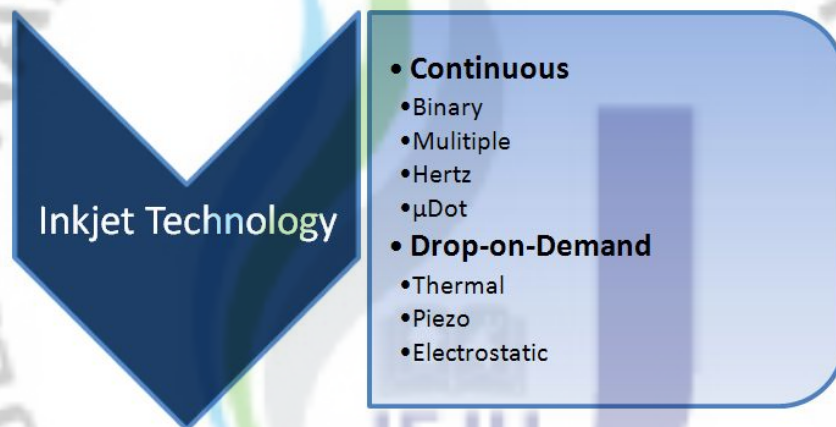


Figure 2.7. Classification of inkjet Technology

As shown in the fig. 2.7 the drop-on-demand printer can be classified into three main categories namely Thermal inkjet (TIJ), Piezoelectric inkjet (PIJ) and Electrostatic Inkjet (EIJ). In the discussion to be followed TIJ, PIJ and EIJ will be discussed briefly.

2.4.1 Thermal Inkjet

A thermal ink-jet consists of an ink chamber having a heater with a nozzle nearby. With a current pulse of less than a few microseconds through the heater, heat is transferred from the surface of the heater to the ink. The ink becomes superheated to the critical temperature for bubble nucleation, for water-based ink, this temperature is around 300°C. When the nucleation occurs, a water vapor bubble instantaneously expands to force the ink out of the nozzle. Once all

the heat stored in the ink is used, the bubble begins to collapse on the surface of the heater. Concurrently with the bubble collapse, the ink droplet breaks off and excels toward the substrate. The ink then fills back into the chamber and the process repeats again.

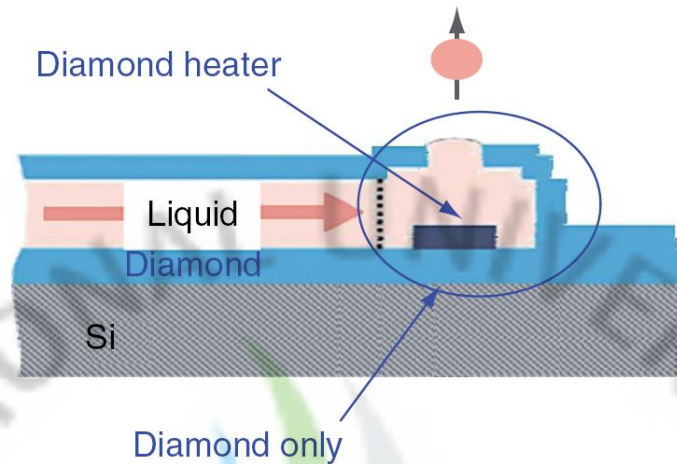


Figure 2.8. Thermal Inkjet: Principle of Operation (Source: Mueller et al. 2005)

2.4.2 Piezoelectric Inkjet

Most commercial and industrial ink jet printers use a piezoelectric material in an ink-filled chamber behind each nozzle instead of a heating element. When a voltage is applied, the piezoelectric material changes shape or size, which generates a pressure pulse in the fluid forcing a droplet of ink from the nozzle. This is essentially the same mechanism as the thermal inkjet but generates the pressure pulse using a different physical principle. Piezoelectric (also called Piezo) ink jet allows a wider variety of inks than thermal or continuous ink jet but the print heads are more expensive. Piezo inkjet technology is often used on production lines to mark products - for instance the use-before date is often applied to products with this technique; in this application the head is stationary and the product moves past. Requirements of this application are a long service life, a relatively large gap between the print head and the substrate, and low operating costs.

2.4.2.1 Squeeze Mode PIJ

A squeeze-mode ink-jet can be designed with a thin tube of piezoceramic surrounding a glass nozzle or with a piezoceramic tube cast in plastic that encloses the ink channel. When a voltage is applied on the piezoelectric material, the ink chamber is squeezed and a drop is forced out of a nozzle.

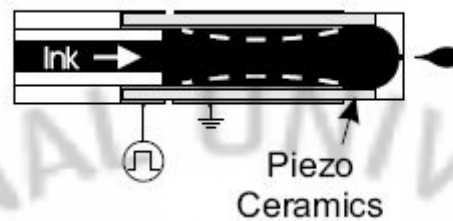


Figure 2.9. Squeeze Mode: Principle of Operation

2.4.2.2 Bend Mode PIJ

In a typical bend-mode design (Fig. 2.11), the piezoceramic plates are bonded to the diaphragm forming an array of bilaminar electromechanical transducers used to eject the ink droplets. The electric field generated between the electrodes is in parallel with the polarization of the piezomaterial.

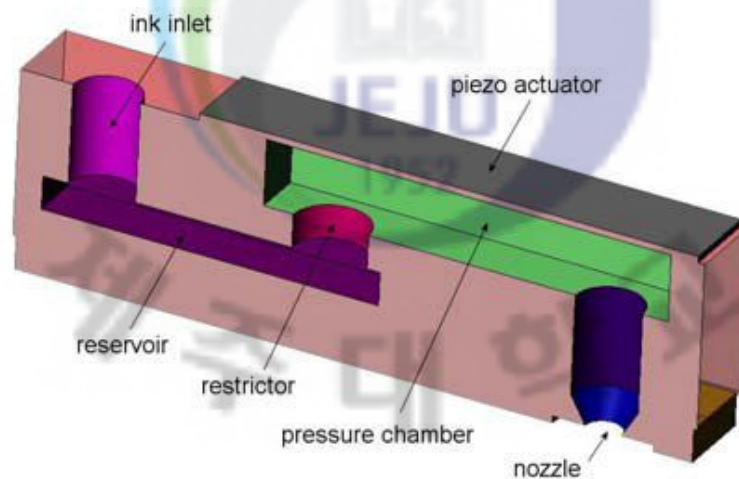


Figure 2.10. Bend Mode: Principle of Operation

2.4.2.3 Push Mode PIJ

In Push-mode design the piezoelectric material is stacked as a rod. As the piezoceramic rods expand, they push against ink to eject the droplets. The electric field generated between the electrodes is in parallel with the polarization of the piezomaterial and since the piezo-ceramic rod is just placed over the ink chamber it provides the necessary ejection force to generate droplet.

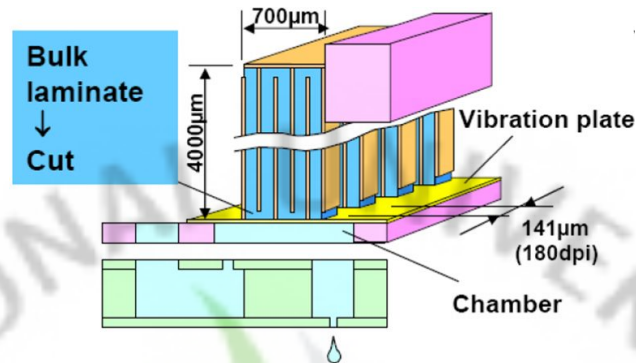


Figure 2.11. Push Mode Inkjet: Principle of Operation

2.4.2.4 Shear mode actuator

The basic operation of a shear mode type inkjet head utilizes the shear mode deformation force of piezoelectric elements. Figure 2.13 shows the working principle of the shear mode piezoelectric actuator. Voltage is applied to the piezoelectric walls on both sides of the ink pressure chamber due to this deformation occurs to both sides of the ink pressure chamber. When the reverse polarity voltage is applied to the piezo walls they apart and ink flows inside the chamber due to the displace volume. A reverse electric field is generated, which makes the nozzle walls curve in the closing direction, delivering ink drops and finally the nozzle walls are returned to initial position.

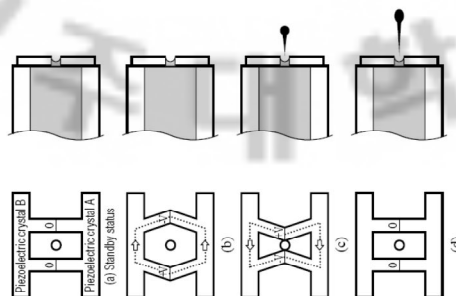


Figure 2.12. Shear Mode Inkjet: Principle of Operation

2.4.3 Electrostatic Inkjet

In electrostatic inkjet operation the driving force for ejecting the droplet is governed by electrostatic potential. Ink chamber is charge with the electrode by applying a positive or negative potential. Whereas the counter electrode is placed just below the nozzle either integrated in the nozzle by means of insulation layer or orthogonal to the nozzle below the printing substrate in a discrete manner. Due to the reverse polarity or grounding effect of the counter electrode ink/liquid in consideration experiences the shear force and forms the cone jet shape which is referred as Taylor cone (Taylor 1969) in literature. Schematic of electrostatic inkjet is shown in figure 2.14 which describe the cone shape being attained by the liquid and other forces which act on the liquid.

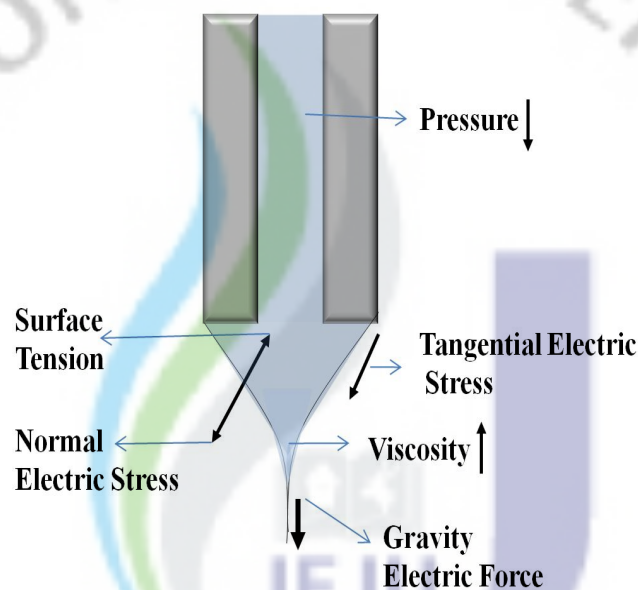


Figure 2.13. Electrostatic Inkjet: Principle of Operation

Conejet shape is attained since the electrostatic potential gradient is orthogonal to the center of the nozzle. Also the electrostatic force increases with cubic of the distance between charge liquid at the interface of the nozzle and the counter electrode.

The main advantage being offered by the electrostatic inkjet printing is the reduced droplet size when compared to the size of the ejection nozzle due to the formation of cone jet during the droplet generation process.

2.4.4 Comparison of Drop-on-Demand Technology

Inkjet printing methods are roughly divided into the piezoelectric type, thermal type and the emerging electrostatic printing. Table 3.2 summarizes the advantages and disadvantages of piezoelectric and thermal type printheads for inkjet printing. Electrostatic printing is still in the development phase therefore comparison of different parameter is difficult to find in literature.

Table 2.2. Comparison of Piezoelectric and Thermal Inkjet Printing

Parameter	Head Type	
	Piezoelectric Type	Thermal Type
Life	Good	Below Average
Print Quality	Good	Average
Power Consumption	Low	Average
Permanent/Disposable	Permanent (replaceable)	Disposable
Reliability	Good	Average
Size	Medium	Small
Cost	High	Low

2.5 APPLICATIONS

Applications of drop-on-demand inkjet ejectors is unlimited and in various field they are mentioned as below (Lee 2003)

Applications in Applied Science

- *Combinatorial Chemistry*
- *Micro-mixing*
- *Automated Micro-titration*
- *Matrix Assisted Laser Desorption Ionization Time Of Flight (MALDI TOF) Spectroscopy*

Sample Loading

- *Loading and Dispensing Reagents from Micro-reactors*
- *Gas Flow Visualization*

Applications in Biotechnology

- *Cell Sorting*
- *DNA Microarrays*
- *DNA Synthesis*
- *Drug Discovery*

- *Medical Therapeutics*

Applications in Manufacturing & Engineering

- *Optics*
- *Droplet-Based Manufacturing*
- *Inkjet Soldering*
- *Precision Fluid Deposition*
- *Displays*
- *Thin Film Coating*
- *Heat Radiators*
- *Monodisperse Aerosolizing for Combustion*
- *Monodisperse Aerosolizing for Dispersing Pesticides*
- *Document Security*
- *Integrated Circuit (IC) Manufacturing*
- *IC Manufacturing — Photoresist Deposition*
- *IC Manufacturing — Conductor and Insulating Dielectric Deposition*
- *Manufacturing — Depositing Sensing and Actuating Compounds*

3 ELECTROSTATIC PRINTING AND MENISCUS GENERATION

3.1 RELATED WORK

Electrostatic inkjet printing stems from the earliest electrohydrodynamic experiment performed by William Gilbert in the seventeenth century which showed the conical shape of the drop when the charged rod is taken closer to the sessile drop. Whereas the stimulus in the electrohydrodynamic research has been fueled by the electrically driven jet paper published in 1969 by Taylor (Taylor 1969). Taylor work opened the avenue for the applications of electrohydrodynamics (EHD) in areas such as electrospraying, dispersion of one liquid in another, coalescence, inkjet printing, boiling, augmentation of heat and mass transfer, fluidized bed stabilization, separation of particles from the mainstream, pumping, polymer dispersion and in biomedical applications (Saville 1997). The fundamental concepts presented by Taylor in 1969 for leaky dielectric model is the touchstone of the present electrostatic inkjet printing. Natural pulsation of the electrically sprayed liquid was also studied in vacuum so that the effect of the gravitation forces is negligible and the pulsating forces are dominated by the electrostatic forces (Carsen et al. 1964, Hendricks et al. 1964, Pfeifer and Hendricks 1968, DeShon and Carson 1968). But their application was limited to electrospray where the accuracy of the droplet on the substrate is of little importance.

In 2002 Murata demonstrated the electrostatic printing of the charge ink droplets smaller than the size of the drops to be printed by any of the former inkjet process. Ultra fine wiring of few microns in width was demonstrated by means of a desktop printing station. Later in 2003 and 2004 Murata demonstrated the super-fine inkjet technology for the fabrication of conductive lines on the substrate printed through the electrostatic printing (Murata 2003, Murata 2004). In 2005 again Murata showed the use of electrostatic printing method to create the micro-bumps (pitch 50 μm and diameter of about 15 μm) and micro wires (Line width 1 μm and pitch of 10 μm) (Murata 2005).

In 2007 Roger's Research group at University of Illinois demonstrated the High-Resolution Electrohydrodynamic Jet Printing for generating the complex electrode geometry and line width of 2 μm with nozzle diameter ranging from 0.3 to 30 μm (Park et al. 2007). In 2008 Ishida research group also demonstrated the inkjet printing method for the printing of water soluble carbon nanotube (CNT) solution. They also demonstrated that the printed drop size of the liquid was reduced by increasing the viscosity of the liquid (Shigematsu et al. 2008). In the same

year Kawamoto at the Waseda University, Japan demonstrated the electronic circuit printing, 3D printing and film formation by means of electrostatic printing. However the print resolution was limited to $30\mu\text{m}$ and the uniformity of the lines was not repeatable for certain experimental parameter (Kawamoto 2007). In 2006 Lee presented the drop-on-demand micro droplet ejector with a pole type ejector by electrostatic driving force (Lee et al. 2006) and later the same device was improved by offsetting the pole outside the nozzle outlet (Kim et al. 2008). Prior to this he also demonstrated theoretically the electrostatic deformation and ejection of the colloid through the layered electrode fabricated device (Lee et al. 2004).

Even after the successful demonstration of the electrostatic printing method for generating the printed conductive lines the method was not commercialized until now for printed electronic fabrication. This is due to the application of high voltage for the ejection of the droplet being reported and high throughput. Most of the above mentioned electrostatic inkjet setup was studied experimentally by charging the ink through metal capillary or using a charging wire inside the needle. Due to the relatively small dimensions of micro-channel inside liquid posses immense surface viscous force and most of the electrostatic force exerted by the charging electrode is absorbed or disseminated due to the viscous forces.

In the work presented in this thesis an electrokinetic ink pumping mechanism is suggested to overcome or subsidize the effect of viscous forces inside the ink chamber when the charging electrode exerts the electrostatic forces to eject the droplet from the nozzle. In addition to the micro-pumping mechanism a hybrid piezoelectric and electrostatic head concept and its numerical study is performed to demonstrate the role of meniscus generation and the benefits which can be harvested by exerting the electrostatic force when the viscous dissipation of the said force is absent at the nozzle outlet.

3.2 ADVANTAGES OF ELECTROSTATIC INKJET PRINTING IN PE

Electrostatic printing provides some benefits when compared with the other drop-on-demand printing and some of them are listed below

- It is possible to achieve different shape of droplet by means of electrostatic inkjet printing rather than the spherical shape through thermal and piezoelectric inkjet printing. This possibility makes it very attractive for applications where the spindle shape drop can be of great importance.
- Since the actuation frequency can be controlled digitally therefore it is possible to print at higher frequencies than thermal inkjet printing.
- This is the only inkjet printing process which can provide smaller diameter of drop than the nozzle size. Droplet diameter half than the size of the nozzle is widely demonstrated in the literature. In some literature higher nozzle diameter to drop ratio is also reported (Murata 2004).
- It is also the only inkjet process which can provide drop-on-demand and continuous printing with the similar or with changes in the printing setup. The constant DC supply can print the lines continuously where as the A/C supply can produce the drop-on-demand printing on the substrate.
- It is also possible to use high viscous printing ink with the electrostatic ink printing. Whereas the piezoelectric printing is limited to viscosity of 20 mpa.s as a printable ink.

3.3 MENISCUS GENERATION AND ITS ROLE

To understand the role of stable meniscus generation or meniscus it is important to investigate the forces which can hinder in the ejection process. For the ejection process two main contributing forces which acts against the droplet generation needs to be overwhelmed are mentioned below

- Viscous force which arises due to the surface forces being offered by the channel
- Surface tension force between the ink and air interface which act against the breakup of droplet
- Dynamic pressure of the liquid inside the nozzle for the ejection of the droplet. This pressure is required to accelerate the liquid at rest and incase of inkjet printer when the ink chamber is at slight vacuum as compared to the atmospheric pressure has its major part in counteracting the forces which drives the liquid.

Fig. 3.1 shows various forces which acts against the droplet ejection process in case of piezoelectric actuation (Le, 1998).

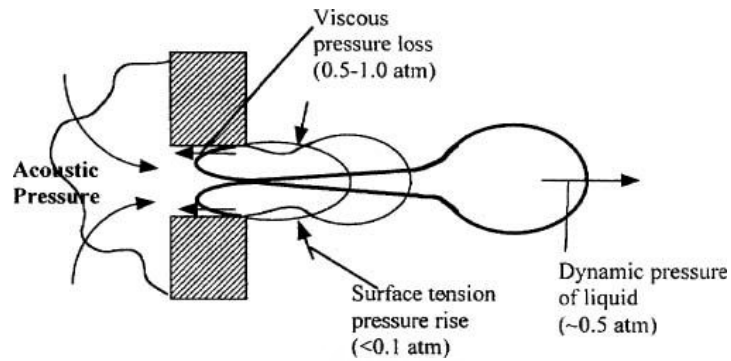


Figure 3.1. Forces acting against the ejection of droplet during piezoelectric actuation

It is evident that none of the above major contributing forces against the droplet ejection can be avoided for the conventional printing method (Thermal and Piezoelectric inkjet methods). The proposed work in this thesis highlights the methodology where the viscous pressure forces acting against the flow of ink can be suppressed or omitted for the electrostatic ejection of the droplet. Such that the meniscus is generated by the help of piezoelectric forces and the liquid is transported at the tip of the ejection electrode which is protrude outside the nozzle. When the meniscus is generated at the tip of the electrode the electrostatic potential is applied which has its highest gradient at the electrode apex. Since the liquid is already outside the nozzle therefore the nozzle viscous forces due to the narrow channel is subsidized considerably. It is also pertinent to mention here that the liquid is accelerated and is transported at the tip of the ejection election therefore the dynamic pressure required to accelerate the liquid at rest is also subsidized. Furthermore, extensive experimental and numerical treatment of the combined effect of piezoelectric and electrostatic actuation can lead to optimized parameter for printing which is out of the scope of the work presented in this thesis due to the lack of manufacturability of the proposed concept in the present laboratory setup.

3.4 PRINTING AND MENISCUS GENERATION STRATEGIES

- I. Constant flow regulated Inkjet Printing
- II. Hybrid Piezo and Electrostatic Printing

3.4.1 Constant flow regulated Inkjet Printing

Flow regulator is one of the essential element of inkjet printer. Many micro drop generation devices and micro-liter flow dependent devices rely on the precise flow rate. The general purpose of these devices is to deliver liquid to the reaction zone or mixing zone (incase of the electrostatic inkjet printer to the electrostatic generating force area from where the droplet can be ejected for printing). To ensure the efficacy of these devices numerical study provides an estimation of physical parameters which results in optimal functionality of the device.

Investigation has been made to evaluate the efficacy of electrokinetic driven micropump through multiphysics based numerical simulation. Parameters such as flowrate and applied electric potential which are responsible for precise flowrate at the outlets of microfluidic device are quantified for horizontal supply channel. Low voltage intensity has been the area of interest in this numerical simulation to govern the flow in microchannel. Due to applied voltage at the interface of microfluidic channel the forces on the particle inside the bulk liquid is unbalanced and provides a net a force in the direction of the flow. This flow transports liquids and samples by electrokinetic effect (electrophoresis, dielectrophoresis and electroosmosis) which is generated through the interaction of the applied electric fields and electrical double layers (EDLs) at the solid–liquid interfaces.

It is envisaged from the numerical study that the small flow rate can be achieved through the electrokinetic effect on the charged particles in the bulk liquid which involves the movement of nano-particles and fluid movement in micro and sub-micro channels due to electric field gradient.

Furthermore, the numerical methodology will be discussed to evaluate the design of electrokinetic driven micropump by considering three cases based on different fluidic channel geometry is discussed and evaluated.

Electrokinetic is an electrically driven motion of particles and fluids. Lab-on-a-chip systems allow designers to create miniature automated, portable, disposable and low cost medical devices. Commercialized Lab-on-a-chip devices generally consists of miniature microfluidic chip to perform the required task where as the other controlling devices are attached to regulate the microfluidic device (A. Kopf-Sill 2000, BH Weigl and P Yager 1998, LJ Kricka 1998, NH Chiem and DJ Harrison 1998, P Yager et al. 1998). The advent of microfluidic technology raises the fundamental question of how to pump and mix fluids at micron scales, where pressure-driven flows and inertial instabilities are suppressed by viscosity (H. A. Stone and S. Kim 2001, Beebe et al. 2002). Most of the work has been done on transporting or mixing the liquid streams from a

certain location to the desired mixing zone, reaction zone or towards the application area (Chen et al. 2003, Zhang et al. 2004, Cummings et al.). Geometries of microfluidic device and application dictates the position and structure of the electrokinetically driven flow device. Often microfluidic application requires disbursement of equal flowrate from the main stream to several or perhaps hundreds of the channel in a continuous supply with similar quantity. This methodology presented herein addresses the microfluidic device mentioned in the later part of the above discussion. The basic aim is to report the difficulties in manufacturability of the horizontal supply channel which disburses the constant flow rate to the vertical channel so that the required fluid can be transported to desired reaction or application region and in the context of this work to the region where electrode charges the ink for generating drop-on-demand droplet through electrostatic force. Numerical simulation of fluid flow with increasing vertical channel width shows that the constant flowrate can be achieved for three or more vertical channels but to manufacture microchannel with such tight tolerance of sub-micron precision and varying dimensions for each channel results in complications. To overcome this problem electrokinetic effect can be introduced to compensate for the differences in the flowrate of the channels.

3.4.1.1 Problem Definition

3.4.1.1.1 Varying Channel Width Geometry with Non-Tapered Supply Channel

A simple microfluidic channel is taken into consideration for the 2D numerical simulation of the fluid flow with two different cases and the electrokinetic assisted coupled fluid flow simulation. Fig. 3.2, Fig. 3.3 and Fig. 3.4 provides the schematic of the numerical simulation being performed for the different cases mentioned above. In all the microfluidic geometry the primary supply channel is horizontal whereas the secondary channel for the delivery or outlets are vertical.

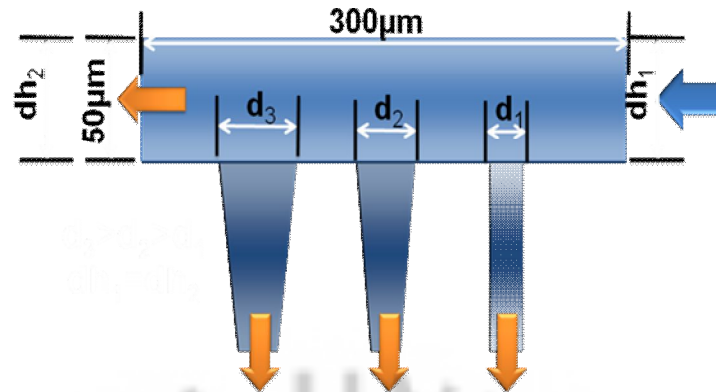


Figure 3.2. Varying Channel Width Geometry with Non-Tapered Supply Channel

3.4.1.1.2 Varying Channel Width Geometry with Tapered Supply Channel

Fig. 3.2 shows the tapered channel geometry. This geometry is similar to the geometry mentioned in Fig. 3.1 except that the primary horizontal channel is tapered thus providing the necessary negative pressure at the opposite side of the horizontal supply to manipulate with the secondary inlet opening as to provide the constant flow at the secondary outlets. The result of the numerical simulation highlights the constant flow across the secondary outlets and is presented in chapter 4 of the thesis.

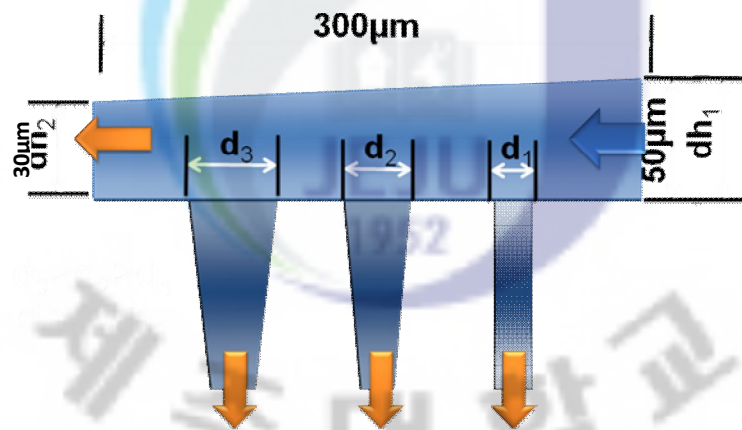


Figure 3.3. Varying Channel Width Geometry with Tapered Supply Channel

3.4.1.1.3 Electrokinetic assisted constant channel geometry

Fig. 3.3 shows the geometry of the electrokinetic assisted microfluidic channel. The primary and secondary channel has uniform geometry which does not change along the length of the channel. Without any electrokinetic force the first channel near the inlet receives the higher fluidic force and the resulting flowrate at the first secondary outlet is higher from the later secondary outlets. To overcome this problem electrodes are introduced at the periphery of the

secondary outlets so to adjust the flowrate on all the secondary outlets without adjusting the geometric dimensions of the fluidic channel. Due to the conductive media the net force induced by the DC electric field drags/repel the nano particle colloidal to compensate the fluidic force being exerted in higher magnitude at the first secondary outlet of the channel.

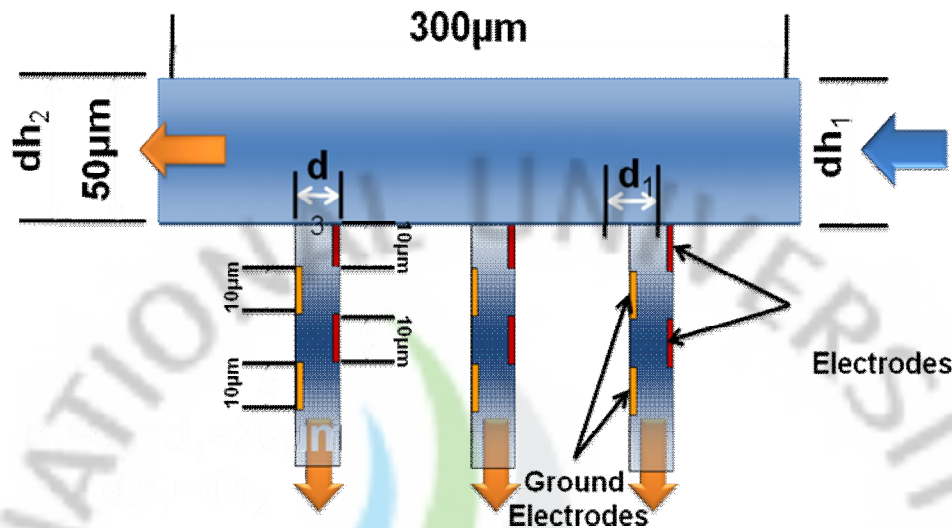


Figure 3.4. Electrokinetic assisted constant channel geometry

3.4.1.2 Electrokinetic Theoretical background

There are various forces acting on the particles moving with the same velocity in the carrying medium under the influence of non-uniform electric field with changing geometry and electrodes separated by a constant distance along the length of the microchannel. When the particle is introduced to the non-uniform electric field the particles experiences a net force in the direction of attracting or repulsive high electric field. This net force drags the colloids and a net flow above or below the pressure regulated flow can be achieved across the channel of the microfluidic device. The direction of the resultant force dictates the additive or subtractive head governed by these forces.

For the numerical simulation using a commercialized finite element package uses the Navier-Stokes equation. The Navier-Stokes equation (Munson et al. 2002) for the incompressible flow can be defined as:

$$\rho \frac{du}{dt} = -\nabla P + \eta \nabla^2 u + \rho g \quad (3.1)$$

The first two cases for the proposed fluidic device are solved using the no-slip conditions at the walls and conservation of mass mentioned by Navier-Stokes equation at Eq. (1). For the

electrokinetic force some electrical stresses needs to be introduced and are mentioned in the terms of mechanical stress including the electric stress as:

$$\rho \frac{du}{dt} = \nabla \cdot (T^m + T^e) \rho g \quad (3.2)$$

Where, T^m is the mechanical stress of the fluid and T^e is the electrical stress (Castellaos 1998) can be written as:

$$\nabla \cdot T^m = -\nabla P + \eta \nabla^2 u \quad (3.3)$$

$$\nabla \cdot T^e = qE \quad (3.4)$$

Where ' E ' and ' q ' are the electric field and electric charge respectively. The effect of the polarization forces are neglected because in isotropic and incompressible fluid the permittivity has no gradient and the dielectric force is also equals to zero (Melcher 1981)

3.4.1.3 Numerical Estimation Parameters

First the numerical simulation has been done for fluid flow in order to quantify the variation of the vertical inlet diameter to achieve the constant flow rate across all three channels. Finally the electrokinetic assisted numerical simulation has been performed to show that the constant flowrate across all three vertical channels can be achieved with same channel opening. Parameters used in the numerical simulation are mentioned in the table below.

Table 3.1. Numerical simulation parameters of the electrokinetic fluidic channels and flowrate for all the microfluidic channel geometries

S.No.	Parameter	Value
1	Permittivity of the ink colloid	$80\epsilon_0$
2	Concentration of nano silver particles	30% w/w
3	Dynamic viscosity of ink	$30e-3 \text{ pa.s}$
4	Reference flow rate	25-200 $\mu\text{l/hr}$
5	Density of ink	1070 kg/m^3
6	Surface Tension	0.07N/m

3.4.2 PIEZOELECTRIC HYBRID INKJET SYSTEM

The drop-on-demand inkjet system having a piezo pressure as a driving force consists of an ink chamber which is then connected with the printing nozzles. The part of the chamber consists of a piezoelectric element that can be excited by a short electrical signal pulse. The excitation caused by the electric signal aligns the neutral distribution of charges due to polarization in the piezo-element and produces the deformation. The deformation thus produces the sudden

change in ink pressure in the chamber, which leads to the ejection of an ink droplet from the nozzle. The chamber is then refilled with ink from an ink reservoir.

In most of the piezo actuated drop-on-demand inkjet system the ink pressure is maintained below the atmospheric pressure when the printer is not in operation. Since the nozzle outlet surface is exposed to the air therefore the meniscus forms, whose slight curvature counterbalances the negative static pressure and results in a stable meniscus within the nozzle. Due to the slight vacuum inside the ink chamber the meniscus remains stable regardless of the wetting surface surrounding the periphery of the nozzle.

The aforementioned DOD system is quite useful for printing intermittent lines and applications where continuous printing is not required. Furthermore, the intermittent nature of the device enables the printing to be done with various inks and pauses as required. During the printing the complex printing can be achieved by moving the printhead (a collection of printing nozzles arranged in an array) relative to the substrate. Due to the nature of the printing it is difficult to achieve smooth curvilinear printing and the printing quality in case of curved path depends on the number of the nozzle being arranged in an array if the other physical printing phenomenon is optimized for a specific task. More specifically such an arrangement of the nozzle determines the printing resolution and is commonly attributed to the number of nozzles per inch (or other length unit) a printhead contains.

Regardless of the resolution of printing the performance of the individual nozzle depends upon the interaction between chamber actuation conditions and the dynamic response of the liquid/ink contained in the system. The interaction between the dynamic response of the piezo-element and ink depends upon various factors such as the air pockets inside the chamber which can absorb the significant amount of pressure especially printing at higher frequency. At higher frequency the possibility of forming acoustic pressure wave harmonics inside the air pocket is high. This is somehow difficult to happen in actual system since the scale of such device is small enough to offer such an interaction. The properties of liquid inside the chamber and surface forces of the chamber are also important factors which can influence the response of the overall system. Quantitatively the quality of the print determines the accuracy of the system which depends upon the drop velocity of ink at the exit of the nozzle and the placement of drop on the substrate relative to the orthogonal line of reference. Moreover the formation of satellite drops (formation of secondary tiny drops during the breakup of liquid) is of main concern and is being controlled by analyzing the printhead design and the excitation frequency of the piezo-element.

3.4.2.1 Problem Definition

The proposed hybrid piezoelectric and electrostatic device is focused on reducing energy requirement for the electrostatic inkjet head with the help of pre-developed meniscus through piezoelectric actuation as mentioned in fig. 3.5. The initiation of the formation of the meniscus with the help of piezoelectric can prove to be helpful for reducing the time to attain the Taylor cone and drop-on-demand inkjet printing. Counter electrode provide the necessary pull force for the generation of droplet size smaller than the size of the orifice opening. The droplet is generated by the help of the step voltage being applied to the electrode layer of the device. It is numerically verified that the conical shape of the electrode provide the highest concentration of the electric field at the tip of the electrode. Since the electrode is extended outside the opening of the orifice; high Maxwell stresses at the tip of the nozzle considerably reduces the applied voltage.

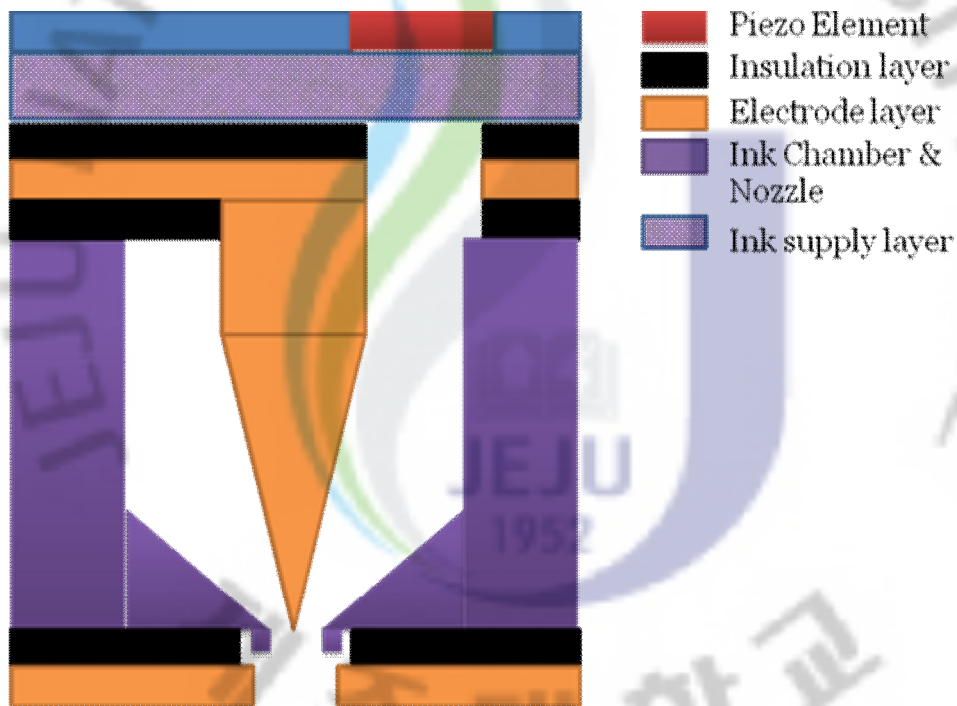


Figure 3.5. Cross-sectional layout of the proposed device

3.4.2.2 Theoretical Background

To understand the piezo-assisted hybrid electrostatic drop-on-demand inkjet printing it is important to disintegrate the hybrid system in to main actuating forces and elaborating them separately.

- a) Piezo-electric Actuation
- b) Electrostatic Actuation

3.4.2.2.1 Piezo-electric Actuation

Piezoelectric material polarizes when it experiences a voltage difference across its layer. The electrical voltage pulse activates the piezoelectric crystal and the deformation produced by the piezo-element generates the pressure wave inside the pressure chamber. The wavefront of the pressure wave is spherical and due to the high value of the bulk modulus of the liquid and relatively smaller dimensions of the ink chamber the propagated pressure is free from harmonics.

The deformation of the piezo-transducer produces the time-variant pressure and velocity field inside the channel structure (Berchtold et al. 1989). This force is designated by the normal acceleration forces at the transducer which is then translated into local and convection acceleration forces and acts against the fluidic viscous forces due to narrow channel and finite pressure propagation resulting from the compressibility. With narrow channel and no-slip conditions at the walls of the channel the fluid velocity profile can be regarded as parabolic. With the parabolic velocity fluidic profile and linear gradient of pressure across the constant cross-section of the nozzle profile the flow can be described by the following pressure forces.

$$P_{meniscus} = P_{dynamic} + P_{viscous} + P_{st} \quad (3.5)$$

Where

$P_{ejection}$ is the pressure required for the formation ink meniscus (in our case not droplet just the meniscus)

$P_{dynamic}$ is the dynamic pressure to actuate the liquid at rest

$P_{viscous}$ is the viscous pressure offered by the walls of the channel

P_{st} is the surface tension force

$$P_{dynamic} = \rho L_n \frac{du}{dt} \quad (3.6)$$

Where,

ρ = density of the fluid

$\frac{du}{dt}$ = change in velocity per unit change in time

L_n = characteristic length of the nozzle

$$P_{viscous} = \frac{8\pi\eta L_n u}{A_n} \quad (3.7)$$

Where,

η = viscosity of fluid

A_n = crosssectional area of the nozzle

$$P_{st} = \frac{2\gamma \cos \theta}{R_n} \quad (3.8)$$

Where,

γ = surface tension of liquid/air interface

R_n = capillary radius

$\cos \theta$ = contact angle of liquid with nozzle

3.4.2.2.2 Electrostatic Actuation

To fully describe the electrohydrodynamic phenomenon of cone-jet it is necessary to indicate the forces acting on the fluid-air interface, stresses being imparted by electrical forces, channel forces and gravitational forces acting on the system in consideration. It is also pertinent to mention here that the electrical properties of the fluid also affect the shearing forces being generated on the charge liquid under the influence of electric field directed towards the exit of the orifice. For instance with perfect conductors or dielectrics the electrical stresses is perpendicular to the interface and alteration of interface shape in the presence of surface tension balances the counter electrical stresses. However, leaky dielectric (which are neither a perfect conductor or dielectric and which is the case being in consideration in this theoretical model) behaves differently due to the presence of free charges which accumulates at the interface of the two-phase liquid (ink and air in this case) alters the electric field. Whereas the viscous effect of the liquid balances the tangential component of the electric field acting of the charged interface.

It is also envisaged that the system in consideration is under the static influence of electric field hence the magnetic phenomenon can be ignored under such condition (Feynman et al

1964). Furthermore influence of electrostatic force is higher than the magnetic force to generate the Taylor Cone therefore electrostatic phenomenon can represent the major of the shearing force.

Fig 3.6. Highlights the aforementioned forces acting on the leaky dielectric media under the influence of electrostatic force.

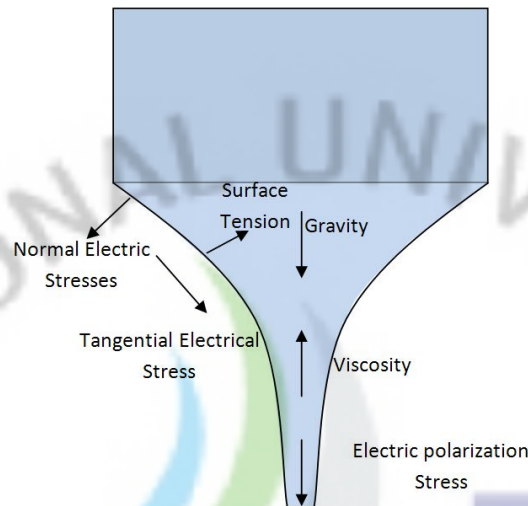


Figure 3.6. Forces acting on the sessile drop under electrostatic forces

Maxwell's equations, simplified for electrostatics states

$$\epsilon_0 \nabla \cdot E = \rho^{(e)} \quad (3.9)$$

and

$$\nabla \times E = 0 \quad (3.10)$$

Where,

E = electric field (The force per unit charge)

$\rho^{(e)}$ = total electric charge per unit volume

ϵ_0 = permittivity of the vacuum

By combining eq. (3.9) and eq.(3.10) and applying divergence theorem for formulating electric field on a closed surface 'S', to the charge 'Q' enclosed in the volume 'V' we have

$$\int E \cdot ndS = \frac{1}{\epsilon_0} \int_V \rho^{(e)} dV = \frac{Q}{\epsilon_0} \quad (3.11)$$

Where n is the outer unit normal.

As electric field is defined as the force per unit charge the force exerted according to the coulomb law is

$$F = E\rho^{(e)} \quad (3.12)$$

From eq. (3.10) the electric field is conservative that is the line integral of $E \cdot t$ (where t is tangent to a closed curve) is zero. Thus there exists a potential function such that

$$E = -\nabla\varphi \quad (3.13)$$

By combining eq. (3.9) and eq.(3.13)

$$\varepsilon_0 \nabla^2 \varphi = \rho^{(e)} \quad (3.14)$$

If the vacuum is replaced by a dielectric medium, the capacity of the charged particles increases because of polarization of the dielectric. Electric fields polarizes the matter in two ways

- By orienting molecules with permanent dipoles
- By deforming electron clouds within individual atoms and molecules

The total electrical force on the liquid is the aggregation of the Maxwell stresses (Electrical forces on free charge) and the electrical polarization force (charge dipoles) is responsible for producing the fluid motion in the electrohydrodynamics (more specifically Taylor Cone phenomenon) under static condition. The dipole force (dielectric force) is represented as

$$F_{dipole} = P \cdot \nabla E \quad (3.15)$$

The polarization vector, P is related to the characteristics of individual dipoles by

$$P = NQd \quad (3.16)$$

Where

N = number of dipoles per unit volume

Q = magnitude of the charge separated to produce the dipole

d = vector indicating the average orientation of the dipole and the charge separation distance

In linear materials. Polarization from the incident field is expressed as

$$P = N\alpha\varepsilon_0 E \quad (3.17)$$

Where

α = polarizability of the atom or molecule (m^3 in SI system)

The dielectric stresses due to polarization of charge particle under the influence of unhomogeneous electric field is referred as

$$T_{dipole} = -\frac{1}{2} |\vec{E}|^2 \nabla \varepsilon \quad (3.18)$$

By combining eq. (3.12) and eq. (3.13) the total electrical stresses per unit volume can be computed as follows

$$T_{\text{Electrical}} = \rho^{(e)} E - \frac{1}{2} |\vec{E}|^2 \nabla \varepsilon \quad (3.19)$$

Eq. 3.19 holds for the condition when the change of electrostatic energy per unit volume doesn't change the pressure inside the liquid. The system in consideration does have some contribution due to this effect. The pressure required to achieve such a case is referred as electrostrictive pressure or stresses and is described as

$$T_{\text{est}} = \frac{1}{2} (\varepsilon - \varepsilon_0) |\vec{E}|^2 \quad (3.20)$$

Maxwell stresses is the combination of electrical stresses and electrostrictive stresses being exerted on the fluid and can be put together as follows

$$T_{\text{Maxwell}} = \rho^{(e)} E - \frac{1}{2} |\vec{E}|^2 \nabla \varepsilon + \frac{1}{2} (\varepsilon - \varepsilon_0) |\vec{E}|^2 \quad (3.21)$$

For incompressible liquid and constant viscosity (η) the motion of the Taylor Cone can be defined by the continuity and momentum conservation equation the system can be defined as

$$\nabla \cdot \vec{u} = 0 \quad (3.22)$$

$$\begin{aligned} \rho \frac{d\vec{u}}{dt} &= -\nabla p + \eta \nabla^2 \vec{u} + T_{\text{Maxwell}} + \rho g \\ &= -\nabla p + \eta \nabla^2 \vec{u} + \rho^{(e)} E - \frac{1}{2} |\vec{E}|^2 \nabla \varepsilon + \frac{1}{2} (\varepsilon - \varepsilon_0) |\vec{E}|^2 + \rho g \end{aligned} \quad (3.23)$$

3.4.2.3 Numerical Estimation Parameters and Approach

Due to the complexity of the numerical estimation of the hybrid piezoelectric and electrostatic concept head the numerical estimation was done discretely and input parameter for the second stage simulation were taken as the initial condition and vice versa. The numerical simulation loop is presented as below

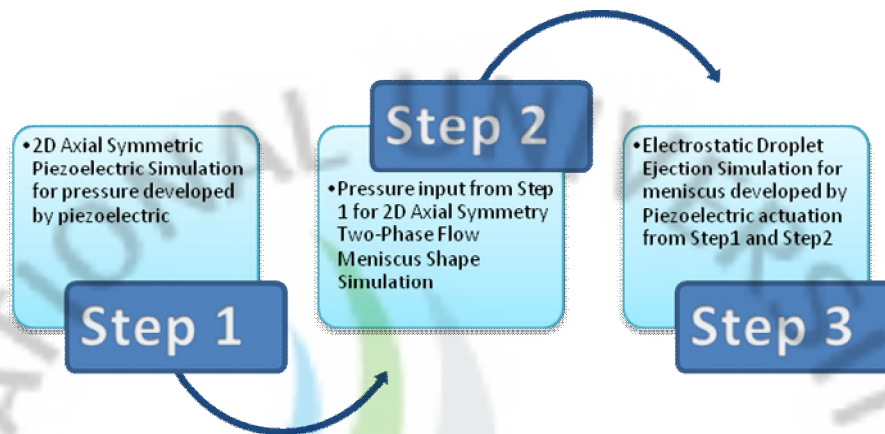


Figure 3.7. Numerical Estimation Step for Piezo-Electrostatic hybrid head

Parameters used in the numerical simulation are mentioned in the table below.

Table 3.2. Numerical simulation parameters for Piezo-Electrostatic hybrid head

S.No.	Parameter	Value
1	Permittivity of the ink colloid	$80\epsilon_0$
2	Dynamic viscosity of ink	$1e-2$ Pa.s
3	Reference flow rate	$225 \mu\text{l/hr}$
4	Density of ink	1000kg/m^3
5	Surface Tension	0.07N/m
6	Dynamic viscosity of air	$1.18e-5$ Pa.s

4 RESULTS AND INTERPRETATION

4.1 VARYING CHANNEL WIDTH GEOMETRY WITH NON-TAPERED SUPPLY CHANNEL

In this type microfluidic channel geometry the numerical simulation is performed for the fluid flow across the primary and secondary fluidic channels. Dimensions of the secondary channel are adjusted such that the first channel has smaller opening than the second channel and vice versa for the third channel. By adhering this philosophy all opening dimensions of the nozzles are adjusted in such a way that the constant flowrate across all the nozzles can be achieved through nozzle channels. Fig. 4.1, Fig. 4.2 and Fig. 4.3 shows the result of the simulation performed at various flowrates.

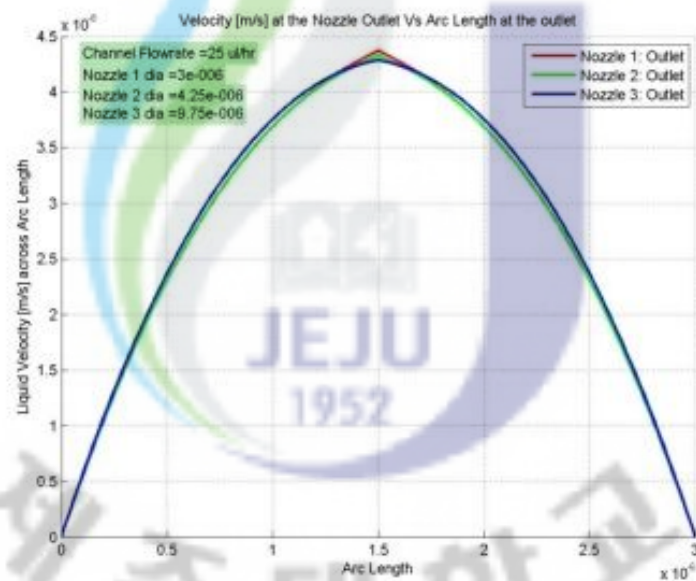


Figure 4.1. Flow simulation for the varying channel width geometry of secondary nozzle with non-tapered primary supply channel. Flowrate across the secondary nozzle for 25 μ l/hr primary channel flowrate

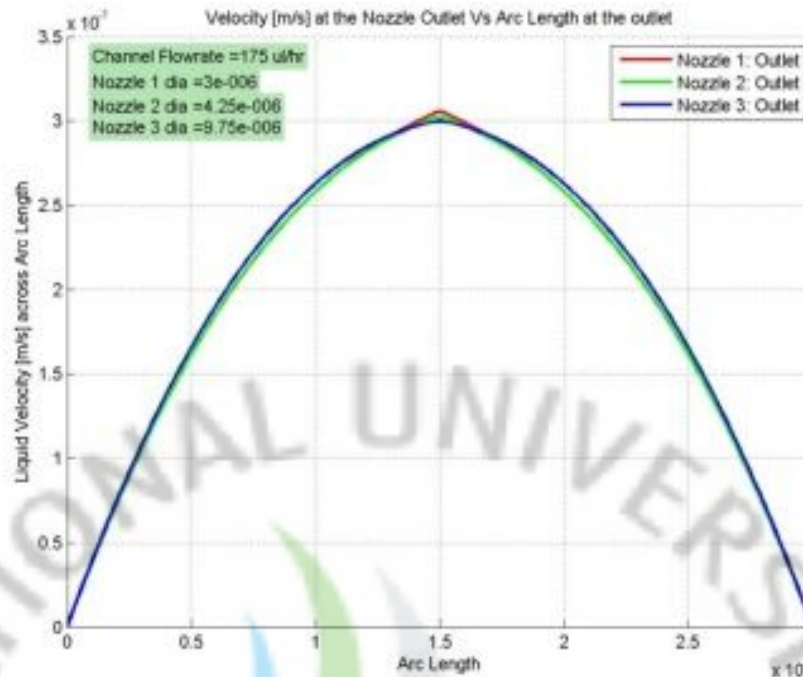


Figure 4.2. Flow simulation for the varying channel width geometry of secondary nozzle with non-tapered primary supply channel. Flowrate across the secondary nozzle for 175 μ l/hr primary channel flowrate

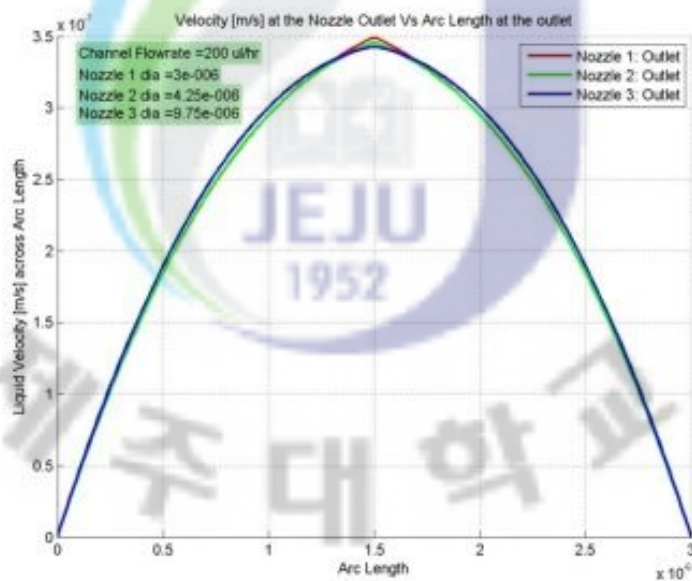


Figure 4.3. Flow simulation for the varying channel width geometry of secondary nozzle with non-tapered primary supply channel. Flowrate across the secondary nozzle for 200 μ l/hr primary channel flowrate.

It is easily interpreted from the numerical simulation that the velocity near the wall of the secondary outlet is zero due to no-slip condition at the walls of the fluidic channel.

4.2 VARYING CHANNEL WIDTH GEOMETRY WITH TAPERED SUPPLY CHANNEL

In this microfluidic channel geometry the numerical simulation is performed for the fluid flow across the primary and secondary fluidic channels. The primary horizontal channel is tapered so to provide the negative pressure along the length of the channel. This causes an increase in the velocity of the fluidic stream thus offering more manipulation to be done with the secondary vertical channel to achieve constant flowrate by offering more opening area starting from the first secondary nozzle to the last as compared with the former case. Results of the flow simulation are highlighted in the figures below.

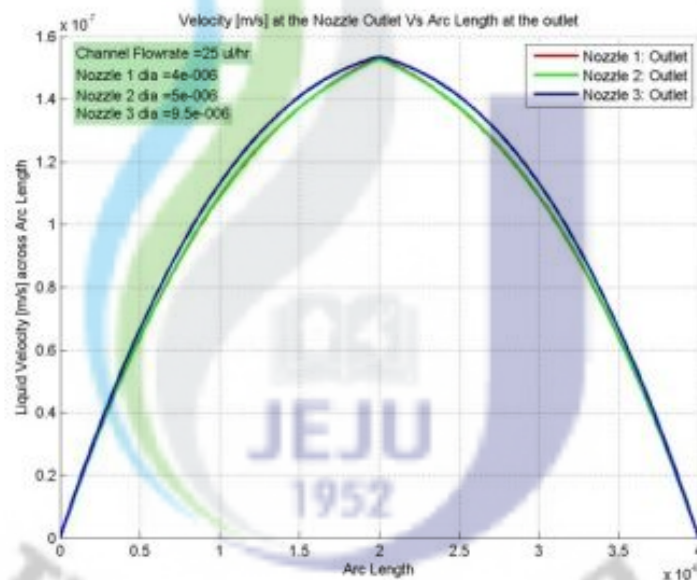


Figure 4.4. Flow simulation for the varying channel width geometry of secondary nozzle with tapered primary supply channel. Flowrate across the secondary nozzle for 25 μ l/hr primary channel flowrate

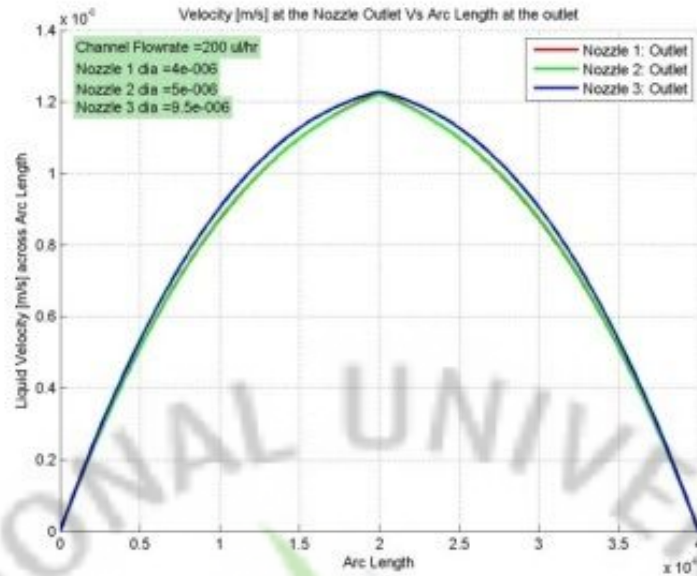


Figure 4.5. Flow simulation for the varying channel width geometry of secondary nozzle with tapered primary supply channel. Flowrate across the secondary nozzle for 175 μ l/hr primary channel flowrate.

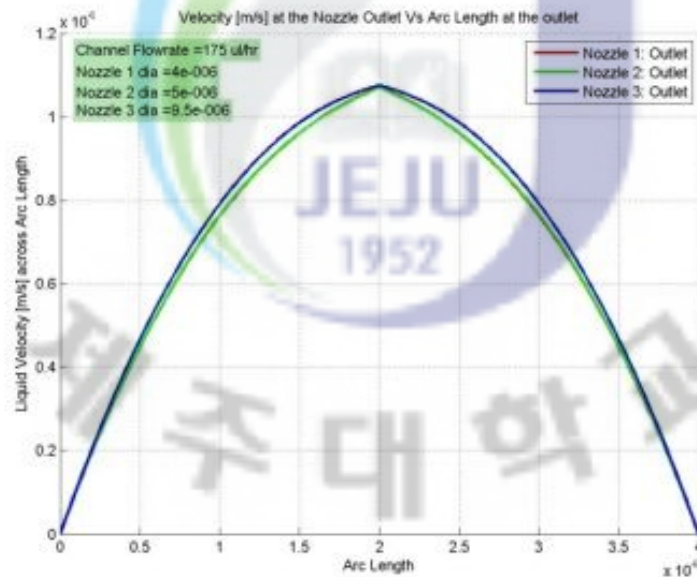


Figure 4.6. Flow simulation for the varying channel width geometry of secondary nozzle with tapered primary supply channel. Flowrate across the secondary nozzle for 200 μ l/hr primary channel flowrate.

4.3 ELECTROKINETIC ASSISTED CONSTANT CHANNEL GEOMETRY

A coupled fluid flow and electric field numerical estimation was performed to signify the electrokinetic driven flow for the conductive colloidal. In this geometry the complexity of numerical simulation is greater and the force balance between the inlet and outlet of the primary and secondary channel varies by both the inlet flowrate and the potential across each electrode of the secondary nozzle. Potential across the electrodes of a particular secondary outlet is kept constant.

Fig. 4.7 highlights the electrostatic field surface profile and streamlines. The surface profile is shown for the simulation performed at $25\mu\text{l/hr}$ primary channel flowrate. It can be envisaged from the surface profile and streamlines that the electric field is stronger at the center nozzle. Fig. 4.8 shows the velocity profile and net electrostatic field at the primary channel of the fluidic device. Due to the strong electric field at the center nozzle the levitation force is being exerted on the primary fluidic channel to suppress the exiting flowrate at the first opening. The appropriate values of the voltages results in the constant flowrate across the secondary outlets. Fig. 4.9 shows the Electrokinetic force which is constant in time domain for the fluidic subdomains.

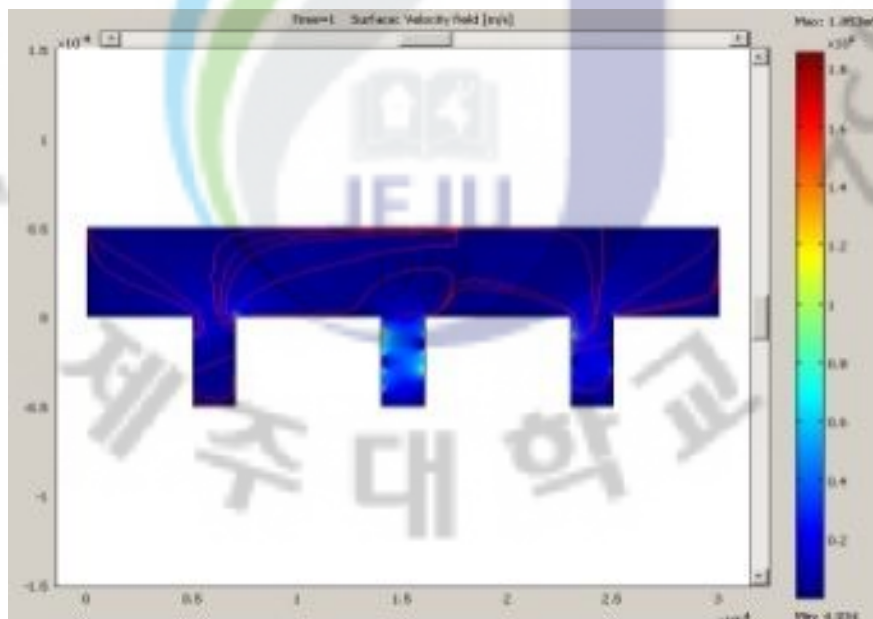


Figure 4.7. Surface gradient of the electric field and streamlines for the electrokinetic flow

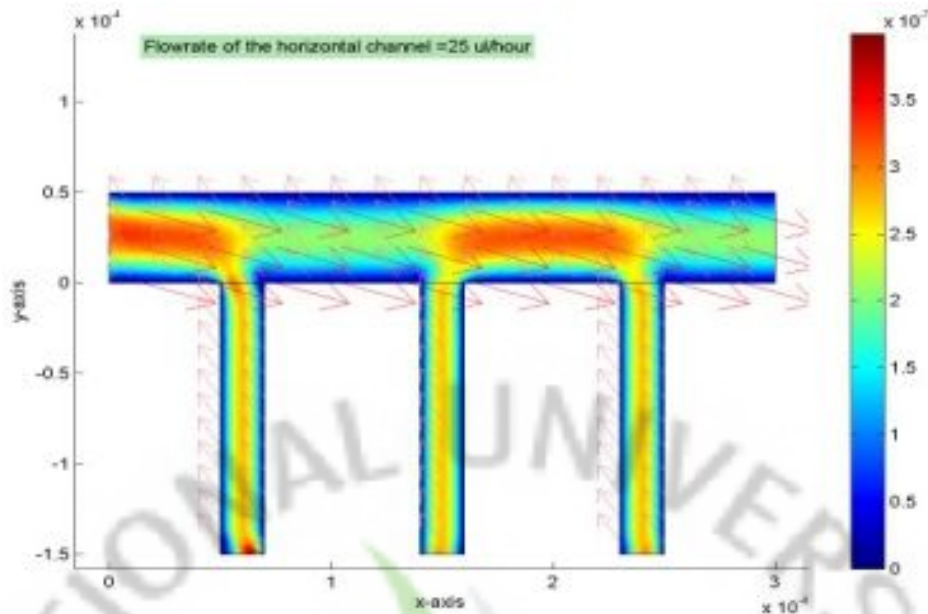


Figure 4.8. Coupled electrostatic and flow simulation for the electrokinetic driven flow from the secondary outlet of the nozzles. Surface velocity profile and electrostatic force direction for the $25\mu\text{l/hr}$ inlet flowrate.

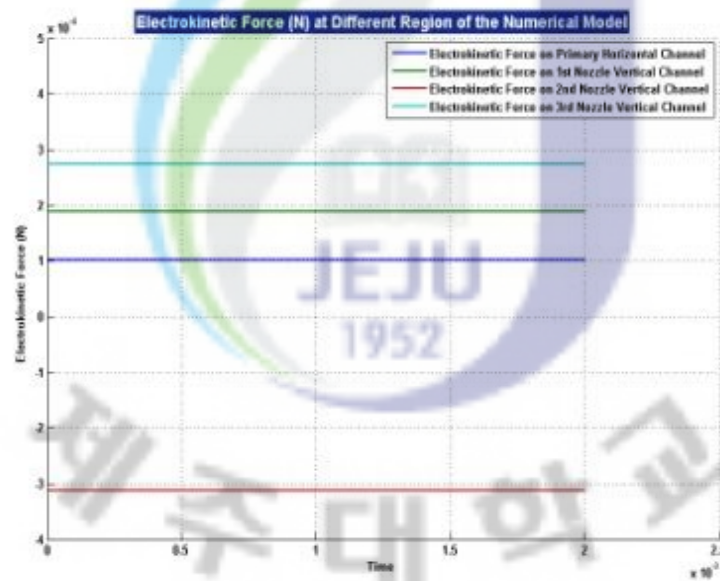


Figure 4.9. Electrokinetic force on different subdomain of the proposed electrokinetic fluidic channel.

Fig. 4.10, Fig. 4.12 and Fig. 4.13 shows the results of the exit flowrates of the proposed electrokinetic fluidic pumping at $25\mu\text{l/hr}$, $175\mu\text{l/hr}$ and $200\mu\text{l/hr}$ inlet flowrate from the primary fluidic channel respectively. It is evident from the figure that the constant flowrate can be achieved through the application of electrokinetic force across the secondary outlets of the channel.

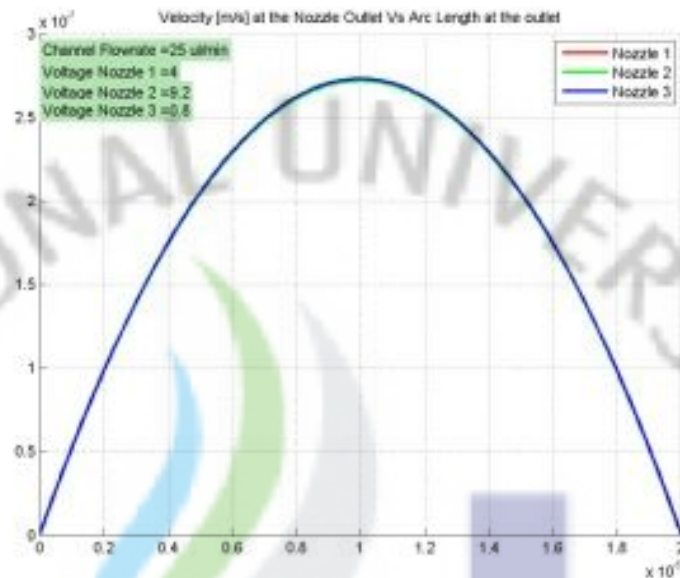


Figure 4.10. Flow simulation for the electrokinetic fluidic pumping channel. Flowrate across the secondary nozzles for $25\mu\text{l/hr}$ primary channel flowrate

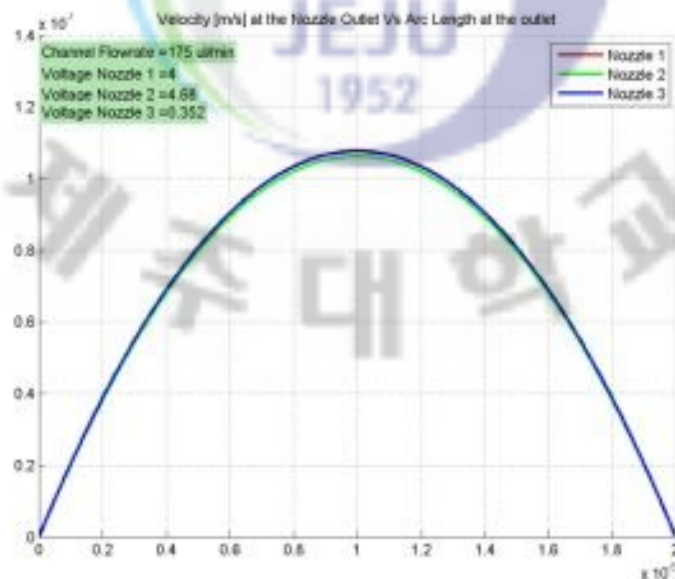


Figure 4.11. Flow simulation for the electrokinetic fluidic pumping channel. Flowrate across the secondary nozzle for $175\mu\text{l/hr}$ primary channel flowrate

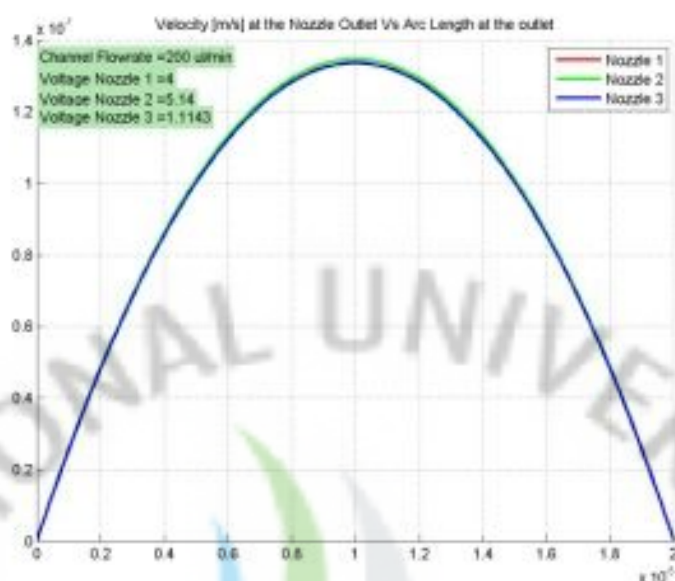


Figure 4.12. Flow simulation for the electrokinetic fluidic pumping channel. Flowrate across the secondary nozzles for 200 μ l/hr primary channel flowrate.

Table 4.1 shows the secondary nozzle sizes of the varying microfluidic channel. It can be easily seen from the table that the tapered channel geometry provides more room for manipulating the fluidic channel and extending the model with more secondary outlets.

Table 4.1. Numerical simulation geometric parameters of the nozzle opening of each geometry.

Geometry	Geometry Parameter		
	d_1	d_2	d_3
Straight Primary Channel	3 μ m	4.25 μ m	9.75 μ m
Tapered Primary Channel (30 μ m primary channel inlet and 19 μ m outlet)	4 μ m	5 μ m	9.5 μ m
Electrokinetic based microfluidic channel	20 μ m	20 μ m	20 μ m

Fig. 4.13 shows the voltage variation across each secondary nozzle to achieve the constant flowrate across the secondary nozzles achieved through electrokinetic as previously shown.

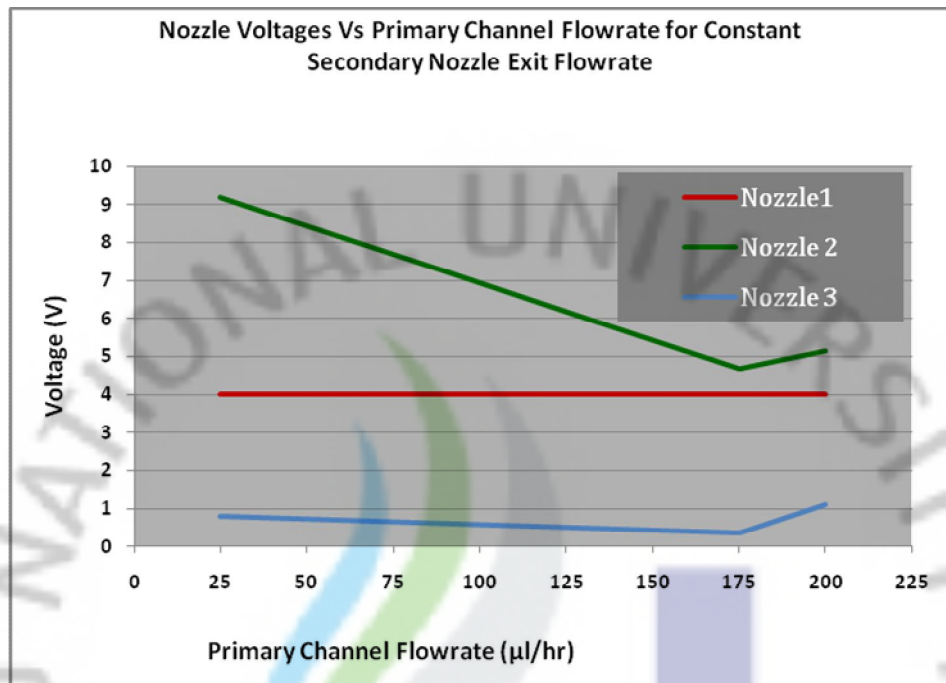


Figure 4.13: Varying voltage at the secondary outlets to achieve the constant flowrate.

4.4 PIEZO-ELECTROSTATIC HYBRID INKJET HEAD

The numerical estimation of droplet generation from the hybrid piezo-electrostatic inkjet head is divided into three discrete simulation and their output are communicated to the second stage of simulation. These steps are divided as follows

1. First the piezoelectric simulation is done to estimate the pressure developed by the piezoelectric actuation in the ink chamber
2. In the second stage of numerical estimation the approximate pressure developed by the piezo-actuator is given as a step pressure function for the two-phase flow meniscus generation simulation.
3. In the end the approximate meniscus shape is taken as the initial liquid/air interface to perform the numerical estimation of droplet generation by means of electrostatic forces.

In the last EHD simulation has been done for a conventional electrostatic inkjet head and the results were compared

4.4.1 Numerical Estimation of piezoelectric pressure generation

Fig. 4.14 and 4.15 shows the step voltage function and numerical parameters of the piezoelectric simulation.

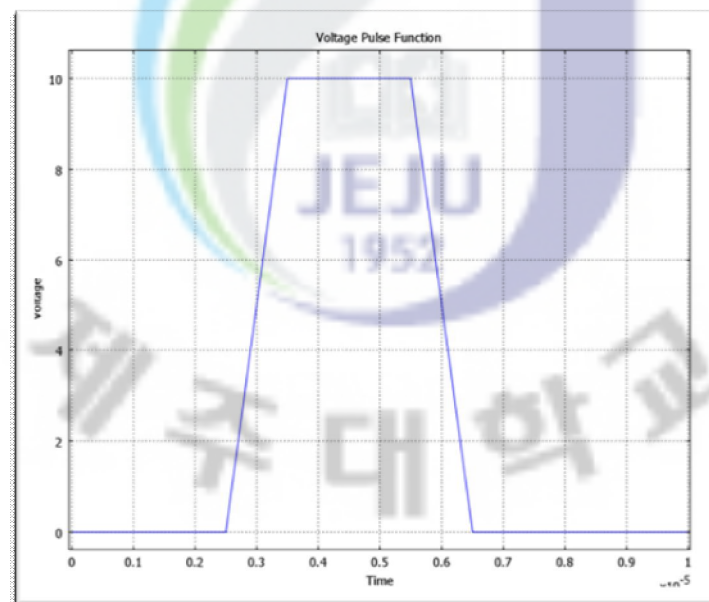


Figure 4.14 Voltage function in domain for piezoelectric numerical estimation

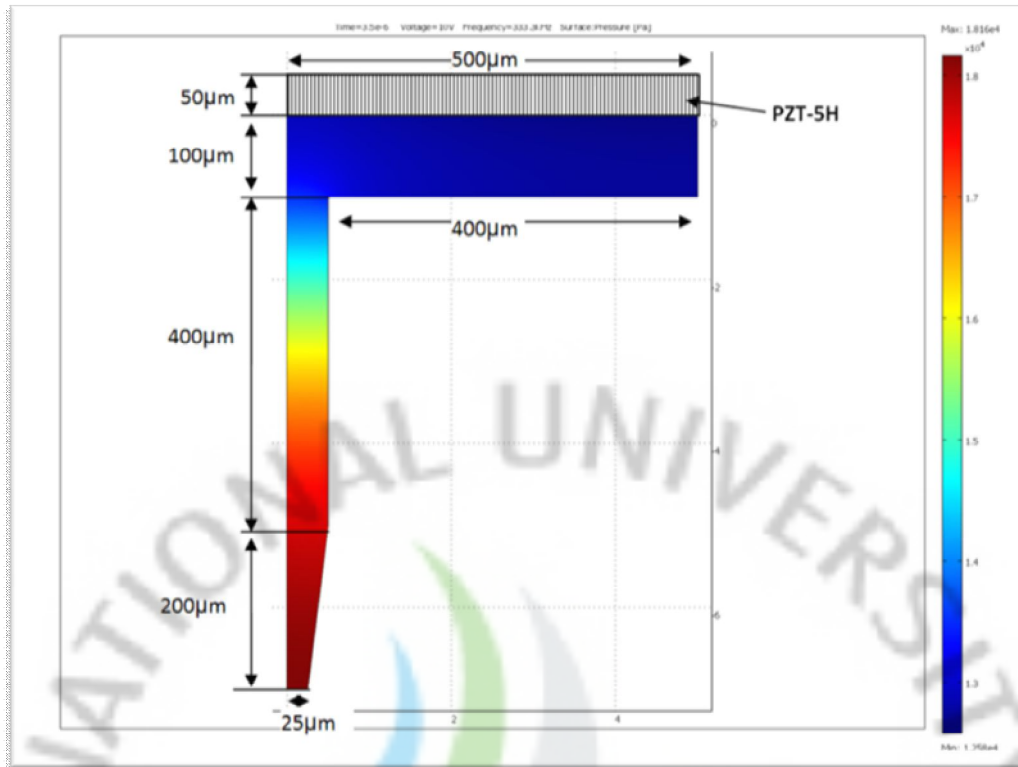


Figure 4.15 Numerical estimation parameters for piezoelectric simulation

Fig 4.16 indicates the pressure generated by means of piezoelectric actuation at different frequencies for a given voltage. The piezoelectric element is polarized by means of the step voltage function being applied at the ink chamber and piezo-element interface. The top part of the piezoelectric element is connected to the ground terminal. When the voltage was applied the piezo-element undergoes deformation which is a function of the applied voltage and frequency. PZT-5H is used as piezoelectric electric element in the numerical estimation of the pressure developed by the piezo-actuator.

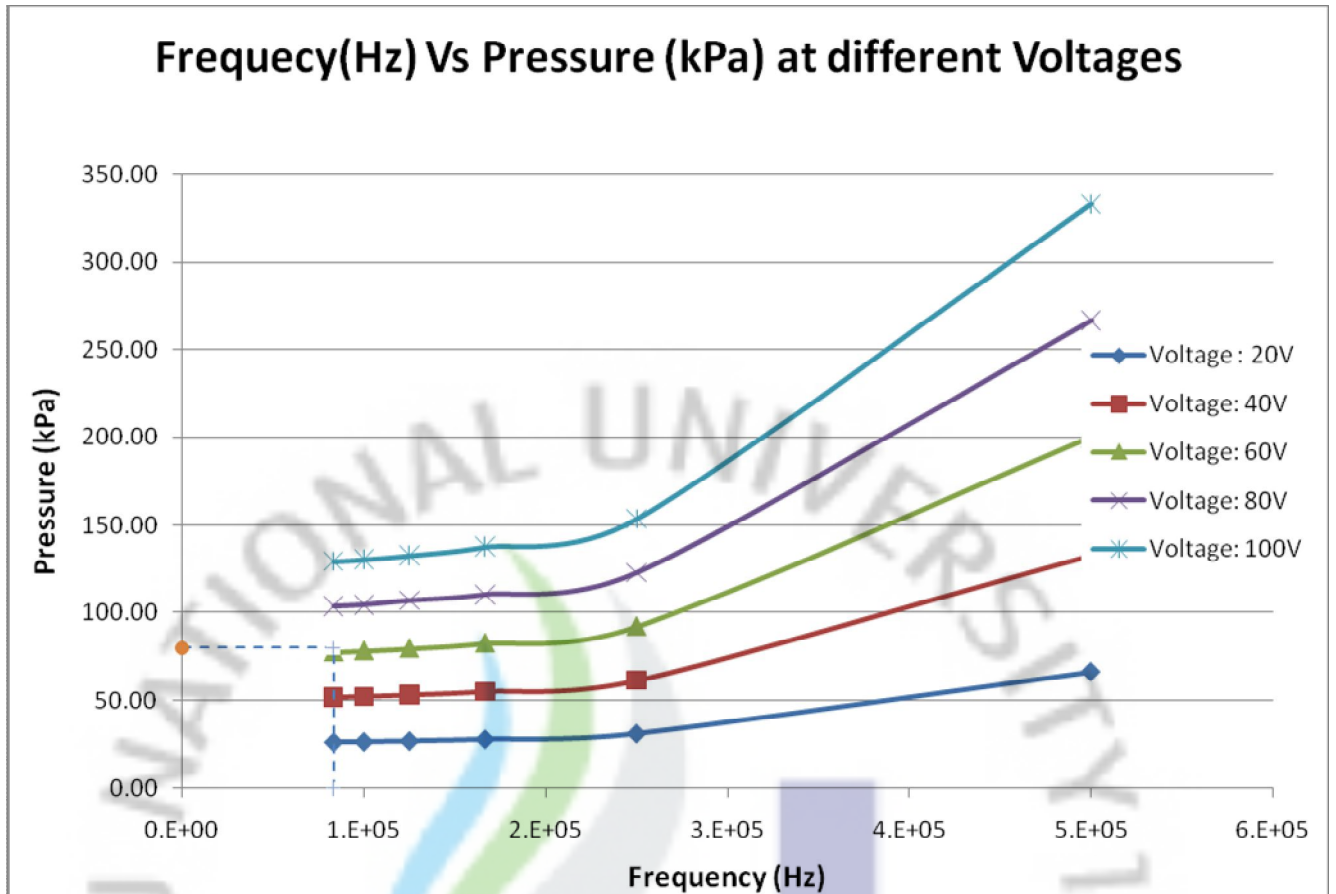


Figure 4.16. Pressure generated in the ink chamber at different frequencies w.r.t. applied voltage

Fig. 4.16 shows that the pressure generated by the piezo-element behaves linearly for the excitation frequency up to 167kHz. Therefore the next step of meniscus generation by means of the piezoelectric actuation is considered the 83.3 kHz frequency response of the piezo-element at 60 volts.

Table 4.2 shows the response of the PZT-5H piezo-element when it has been excited by the voltage function mentioned in fig 4.14.

Table 4.2. Response of PZT-5H

Voltage	Deformation(μm)	Pressure (kPa)	Frequency (kHz)
20	5.62E-08	25.90	83.3
40	1.12E-07	51.80	
60	1.69E-07	77.68	
80	2.25E-07	103.58	
100	2.81E-07	129.48	
20	5.62E-08	26.14	100.0
40	1.24E-07	52.26	
60	1.69E-07	78.40	
80	2.25E-07	104.52	
100	2.81E-07	130.66	
20	5.63E-08	26.58	125
40	1.13E-07	53.14	
60	1.69E-07	79.72	
80	2.25E-07	106.82	
100	2.81E-07	132.86	
20	5.64E-08	27.56	167
40	1.13E-07	55.14	
60	1.69E-07	82.70	
80	2.26E-07	110.26	
100	2.82E-07	137.82	
20	5.68E-08	30.76	250
40	1.14E-07	61.50	
60	1.71E-07	92.26	
80	2.27E-07	123.02	
100	2.84E-07	153.76	

4.4.2 Numerical Estimation of Meniscus generation

After generating the ink chamber pressure by means of the piezo-electric actuation the same needs to be applied to the ink surface at the inlet of the nozzle. This inlet pressure helps the ink to move out of the nozzles and wets the surface of the electrode which is protruded around $20\mu\text{m}$ of the nozzle. Fig 4.17 describes the geometry of the model used for the simulation of meniscus generation by the help of piezoelectric actuation. After wetting the electrode the pressure pulse is removed and the liquid rest momentarily, making a very stable meniscus shape outside the nozzle out. Due to the formation of the meniscus outside the nozzle the surface viscous forces of micro-channel is reduced considerably. At this stage the electrostatic pulse can be used to generate the droplet.

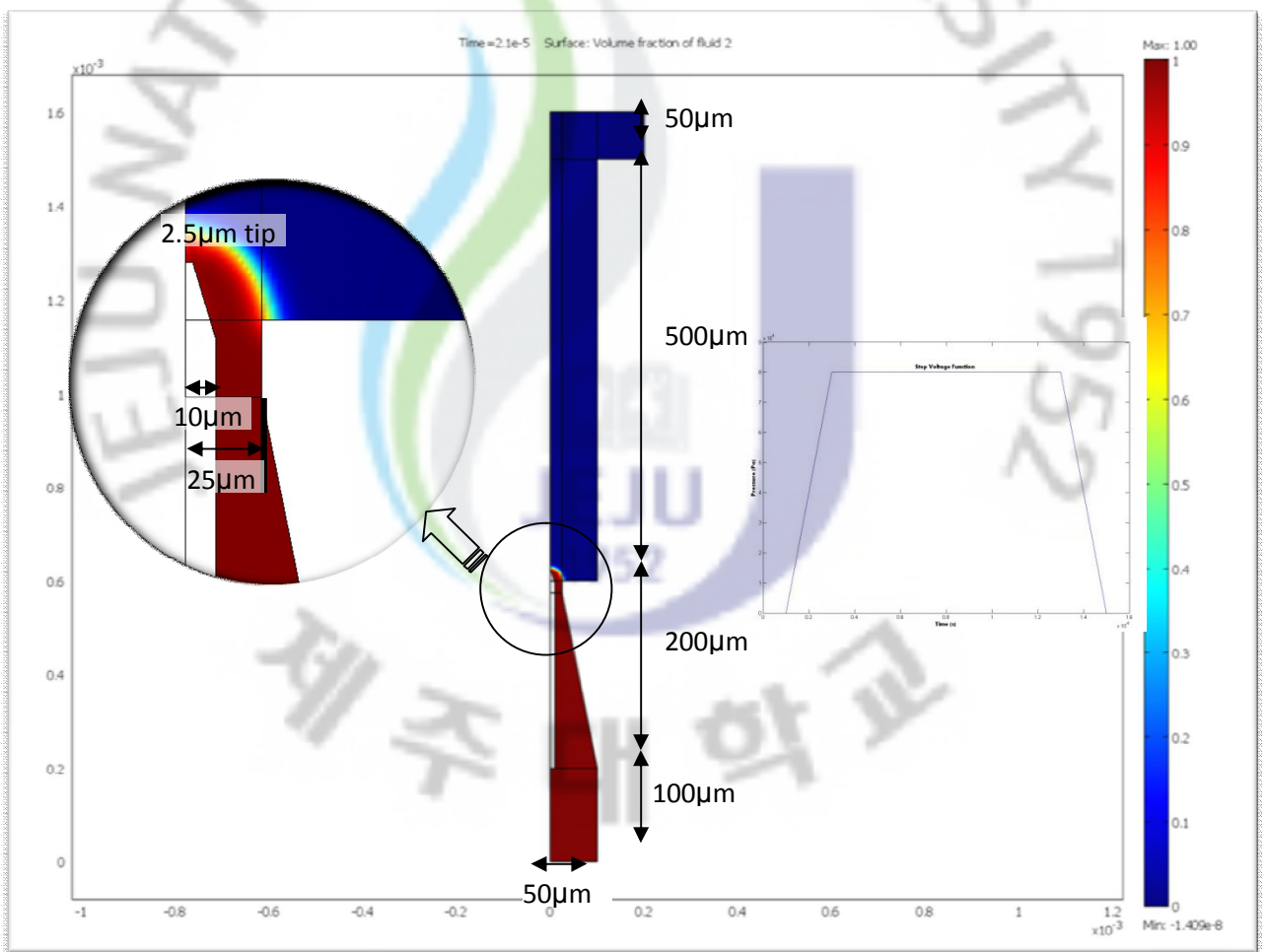


Figure 4.17. Numerical estimation parameters for Two—Phase flow meniscus generation simulation

Fig. 4.18 shows the development of meniscus when the pressure is applied at the nozzle inlet by means of piezoelectric actuation. The pressure force is applied for the first $12\mu\text{s}$ and after

that the force is removed. Since the liquid accelerates due to the applied pressure the meniscus is developed for another $12\mu\text{s}$ and at $24\mu\text{s}$ a stable meniscus is being achieved and shown below.

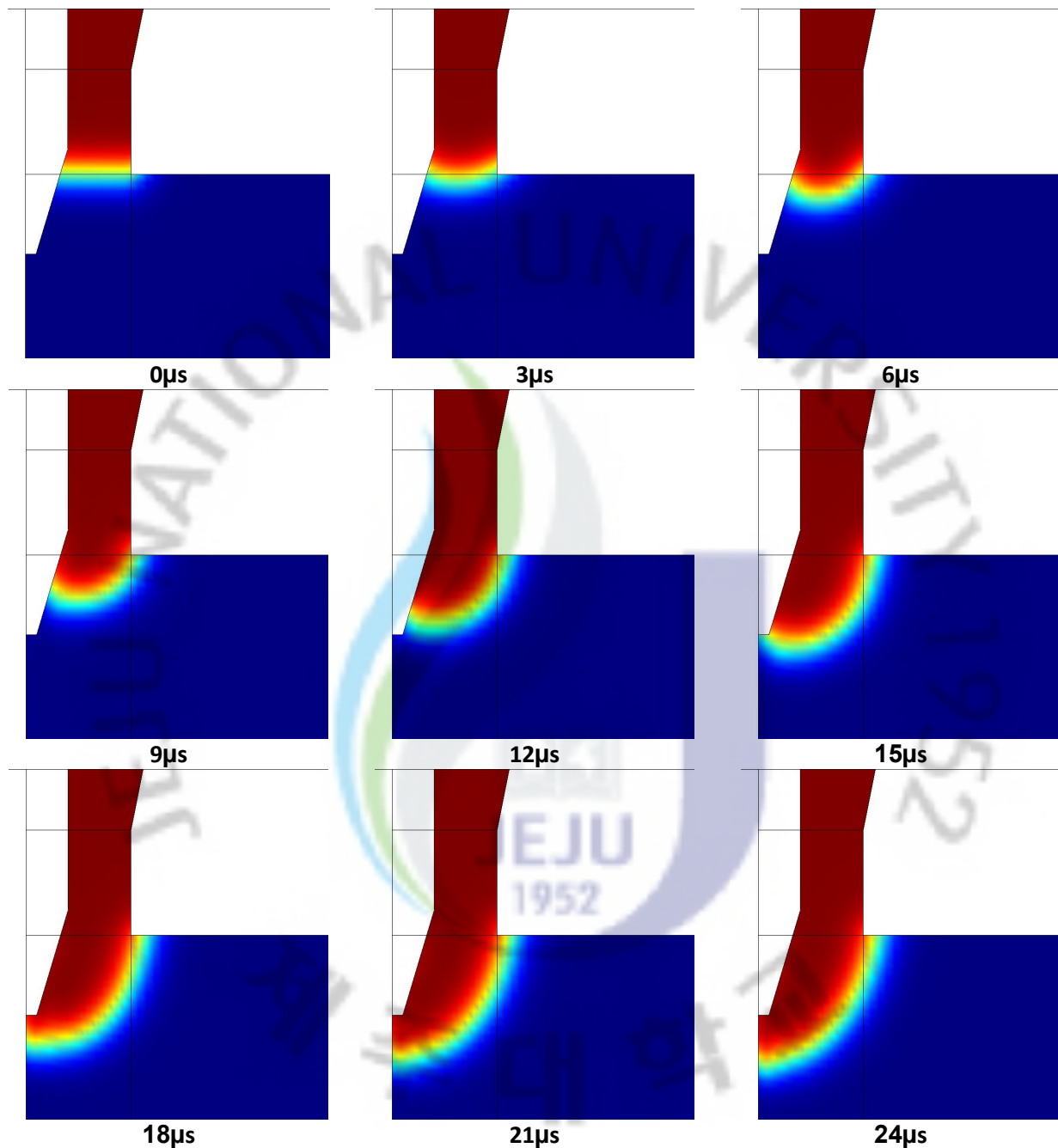


Figure 4.18. Meniscus generation by means of piezo generated pressure in time domain at every $3\mu\text{s}$

In Fig. 4.18 the shape of the meniscus shown for 80kPa pulse pressure being applied by means of the piezoelectric actuator which gives the complete wetting of the electrode being protruded outside the nozzle. Whereas the height of meniscus for different applied pulsed

pressure is also calculated and is shown in Fig. 4.19. It is worthwhile to mention here that the pulsed pressure greater than 60kPa can wet the electrode protruded outside the nozzle outlet.

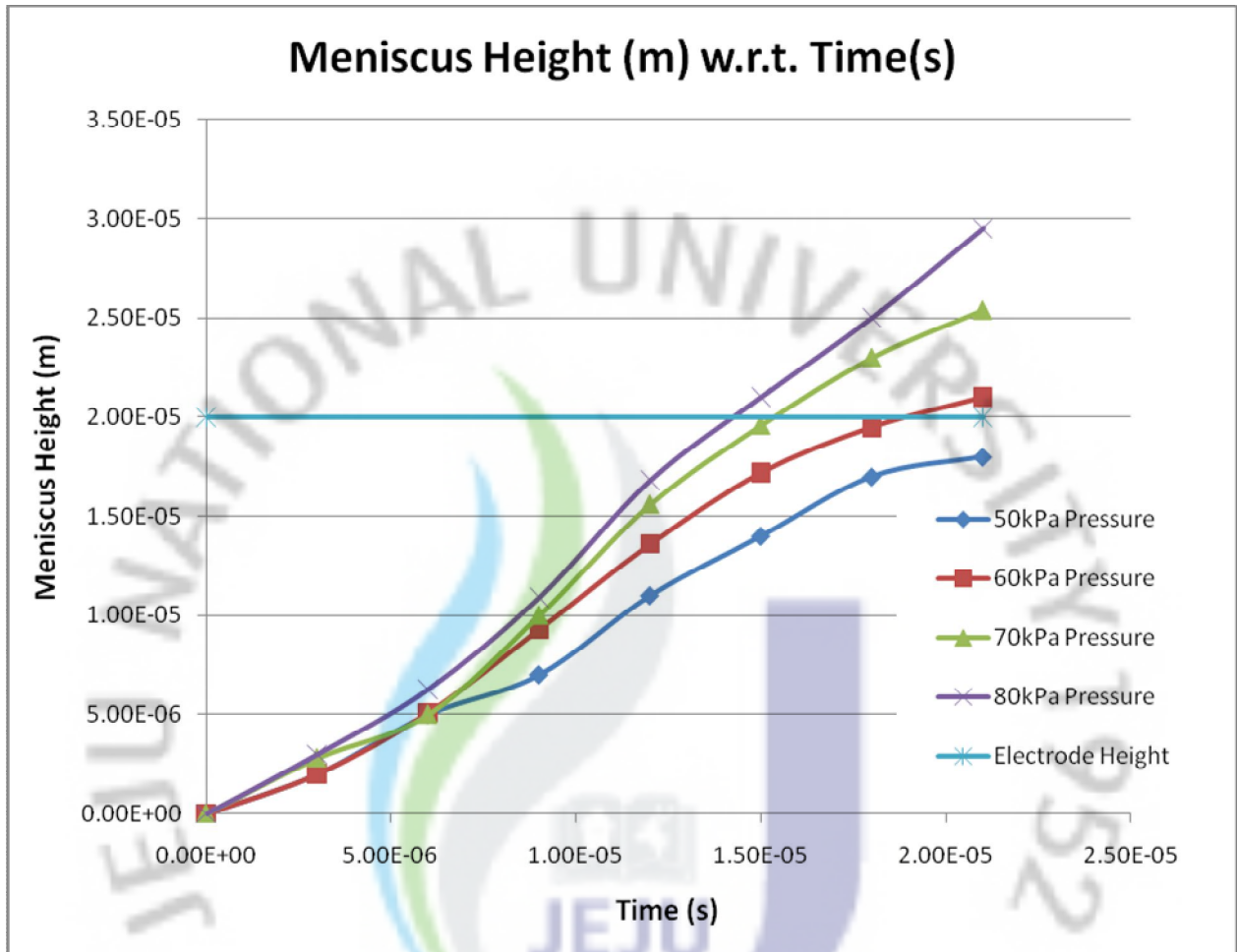


Figure 4.19. Meniscus height in time domain w.r.t. applied pressure through piezoelectric actuator

4.4.3 EHD numerical estimation of pre-developed meniscus droplet generation

After generating the meniscus by means of piezoelectric simulation an estimated shape of the meniscus can be drawn for the two-phase flow electrohydrodynamic (EHD) simulation of droplet generation. Fig 4.20 the numerical simulation geometry and the voltage pulse function.

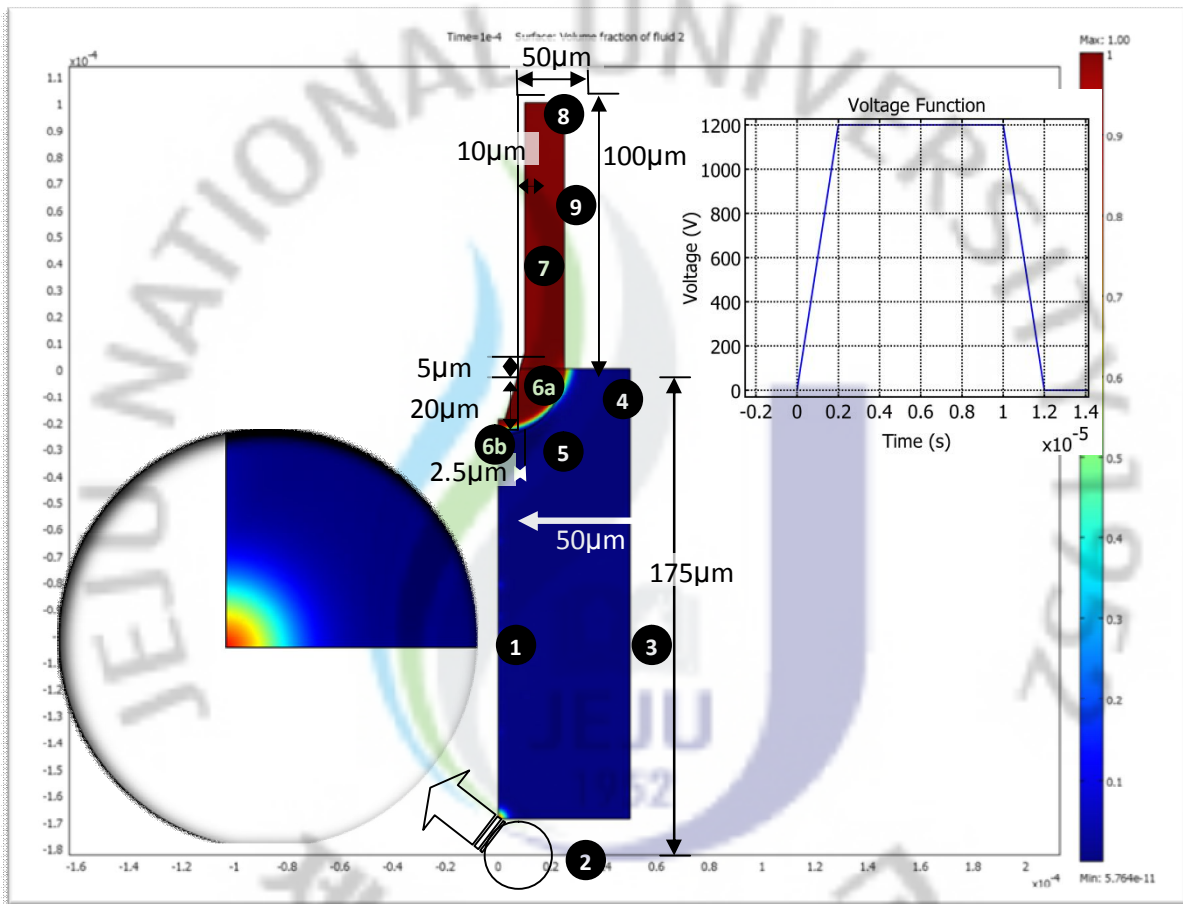


Figure 4.20. Numerical parameters for Meniscus Generated EHD Simulation

Table 4.3. Boundary Conditions for Meniscus Generated EHD Simulation

Boundaries	Condition	Mode
1	Axis Symmetry	
2, 6a, 6b	Wetted walls	
3,4,9,7	No slip	Two-Phase Flow
8	Inlet	
5	Air/Liquid Interface	
6a,6b,7	Electric Potential	
2	Ground	Electrostatics Generalized
3,4,9,8	Insulation/Zero Charge	

Table 4.3 enlists the boundary condition used for the numerical simulation of EHD. Fig. 4.21 shows the formation of conejet shape due to the applied electrostatic potential. The electrostatic potential is applied for the first $12\mu\text{s}$. Different stages of droplet formation are shown below.

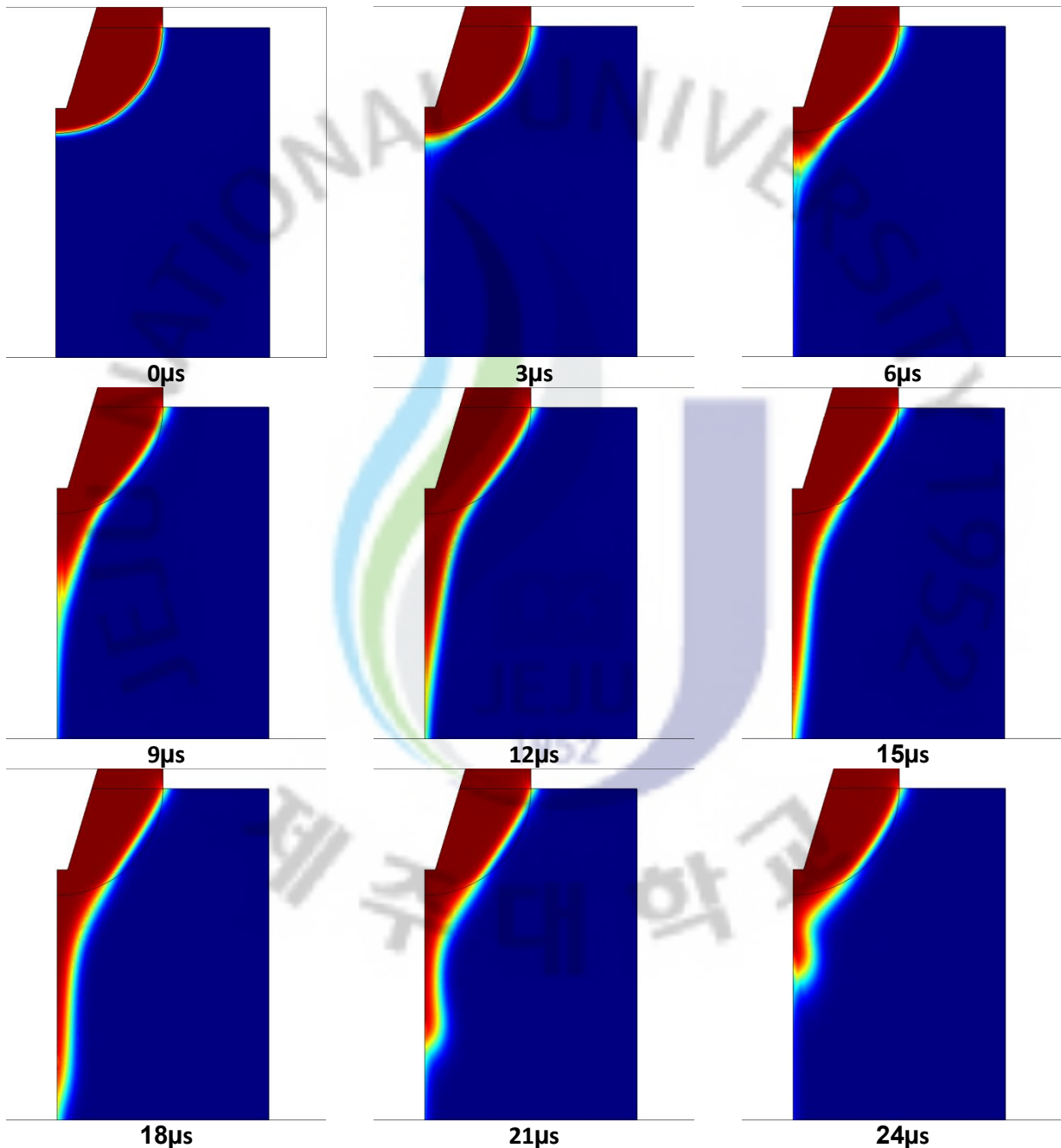


Figure 4.21. Droplet generation in time domain for pre-developed meniscus through piezoelectric actuator

4.4.4 EHD numerical estimation of without meniscus developed droplet generation

To signify the advantage of generating the droplet by means of pre-developed meniscus it is necessary to compare the proposed droplet generation concept needs to compared with the conventional electrostatic inkjet process. Fig. 4.22 illustrates the numerical simulation model and geometry of the model for comparison.

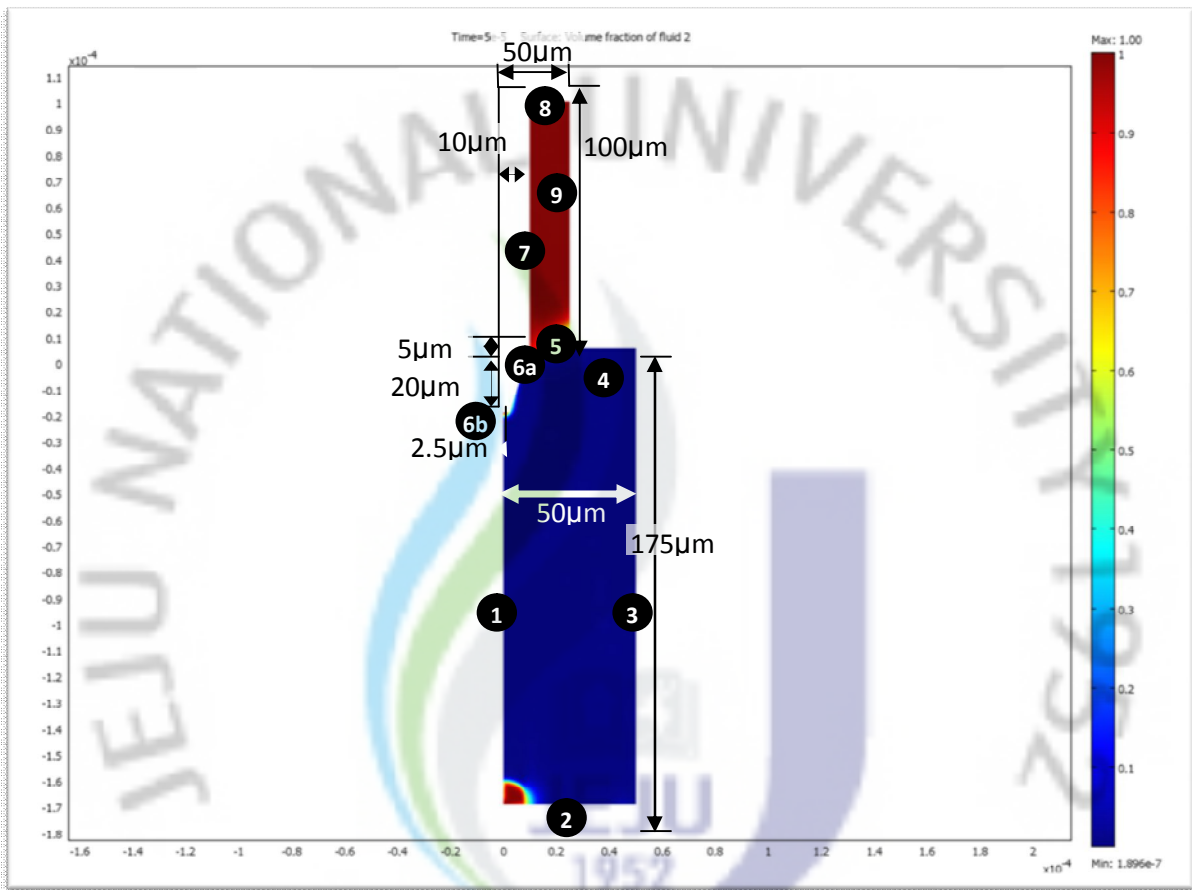


Figure 4.22. Numerical parameters for without Meniscus Generated EHD Simulation

Table 4.4. Boundary Conditions for conventional Electrostatic Inkjet Simulation

Boundaries	Condition	Mode
1	Axis Symmetry	
2, 6a, 6b	Wetted walls	
3,4,9,7	No slip	Two-Phase Flow
8	Inlet	
5	Air/Liquid Interface	
6a,6b,7	Electric Potential	
2	Ground	Electrostatics Generalized
3,4,9,8	Insulation/Zero Charge	

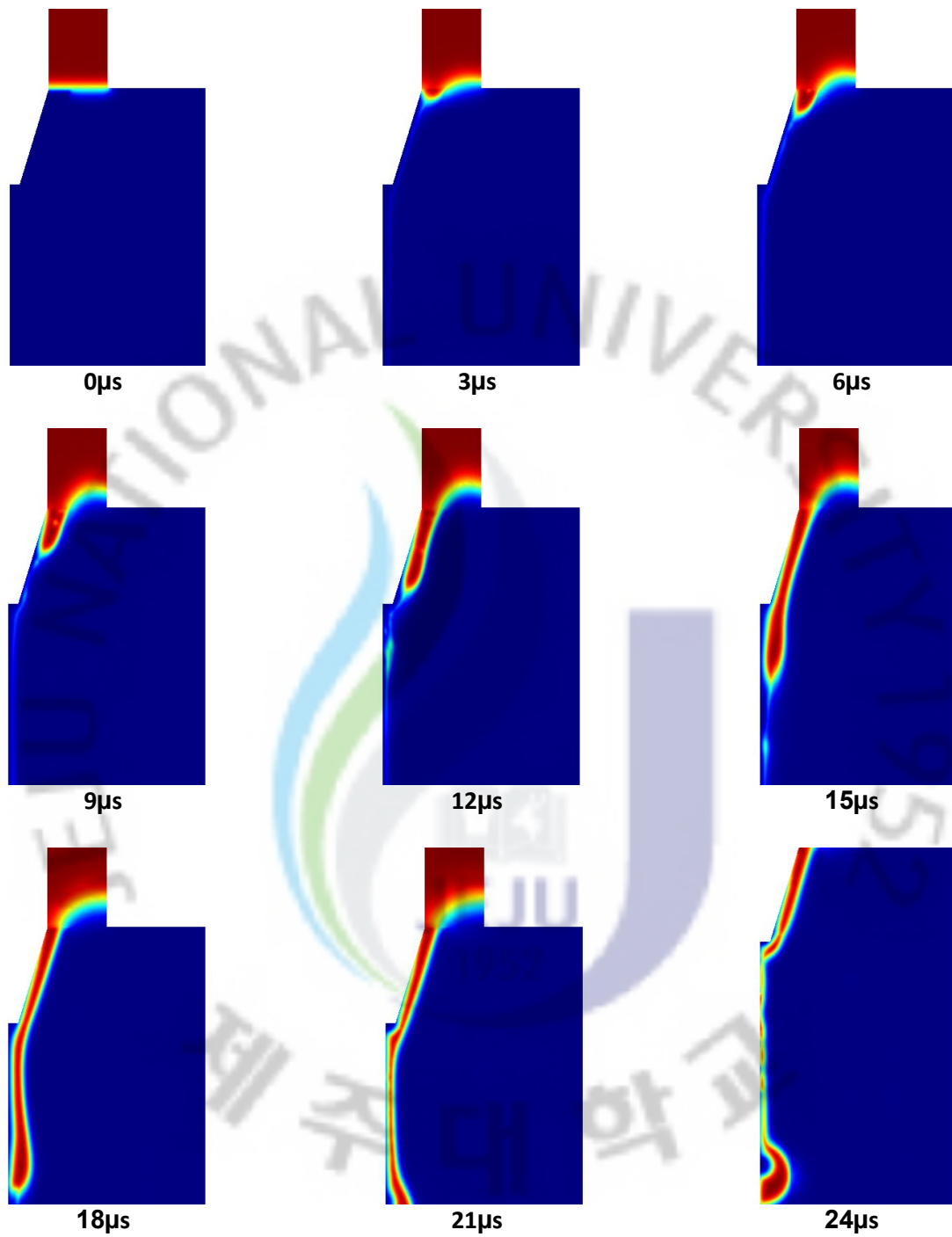
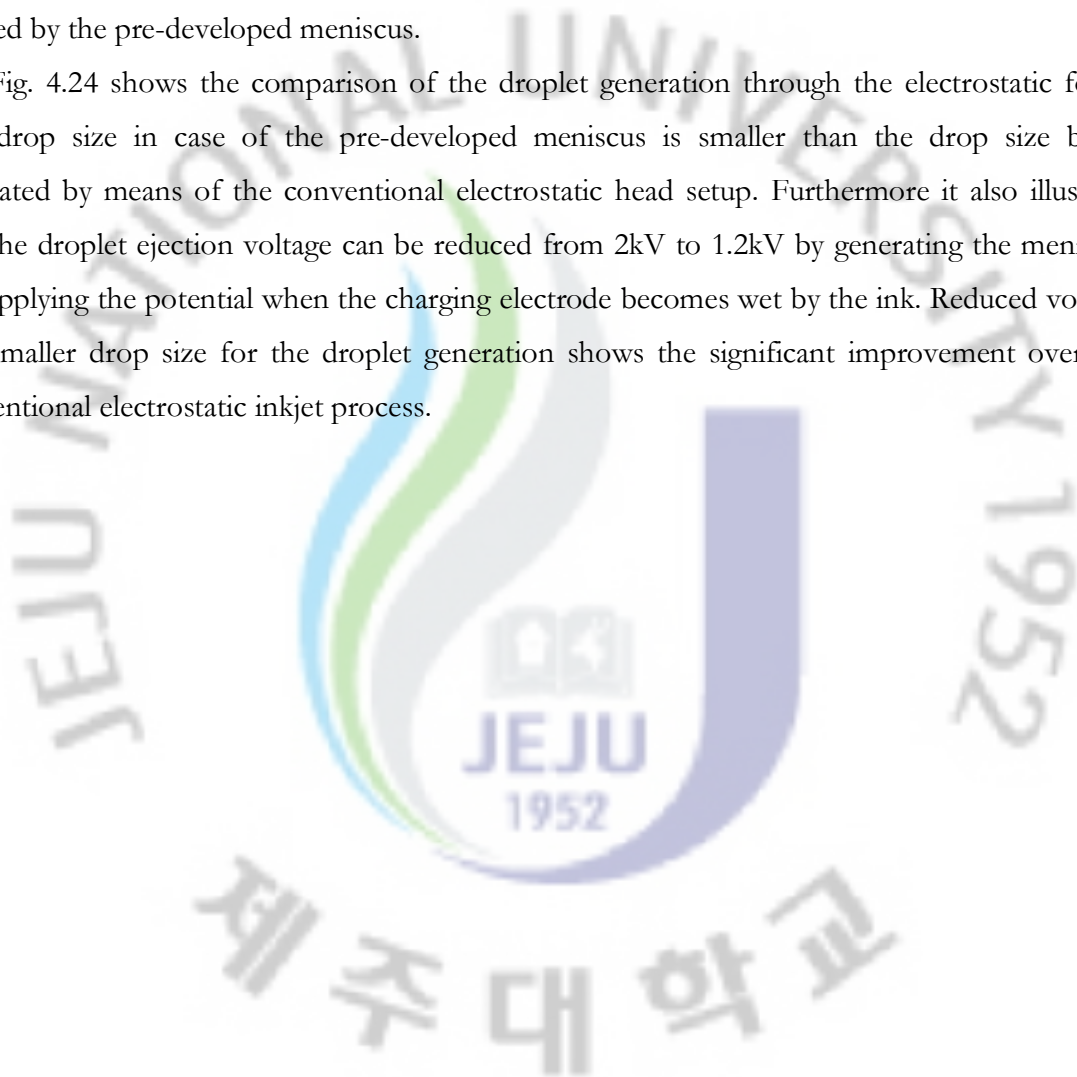


Figure 4.23. Droplet Generation process in Electrode Protruded conventional Electrostatic Inkjet Head

Fig. 4.23 shows the droplet generation process of a conventional electrostatic inkjet head. The simulation shows that the size of the generated droplet is large and the electrostatic ejection pulse required for the ejection of the droplet is long. Since the dynamic pressure needs to accelerate the liquid inside the nozzle is high due to the viscous forces of the nozzle microchannel and the electrode itself. When the droplet is accelerated with the high electrostatic potential the jet diameter formed is thick and inertial forces are high. The combined effect of high electrostatic potential and inertial effect forms the droplet of bigger diameter than the one formed by the pre-developed meniscus.

Fig. 4.24 shows the comparison of the droplet generation through the electrostatic force. The drop size in case of the pre-developed meniscus is smaller than the drop size being generated by means of the conventional electrostatic head setup. Furthermore it also illustrate that the droplet ejection voltage can be reduced from 2kV to 1.2kV by generating the meniscus and applying the potential when the charging electrode becomes wet by the ink. Reduced voltage and smaller drop size for the droplet generation shows the significant improvement over the conventional electrostatic inkjet process.



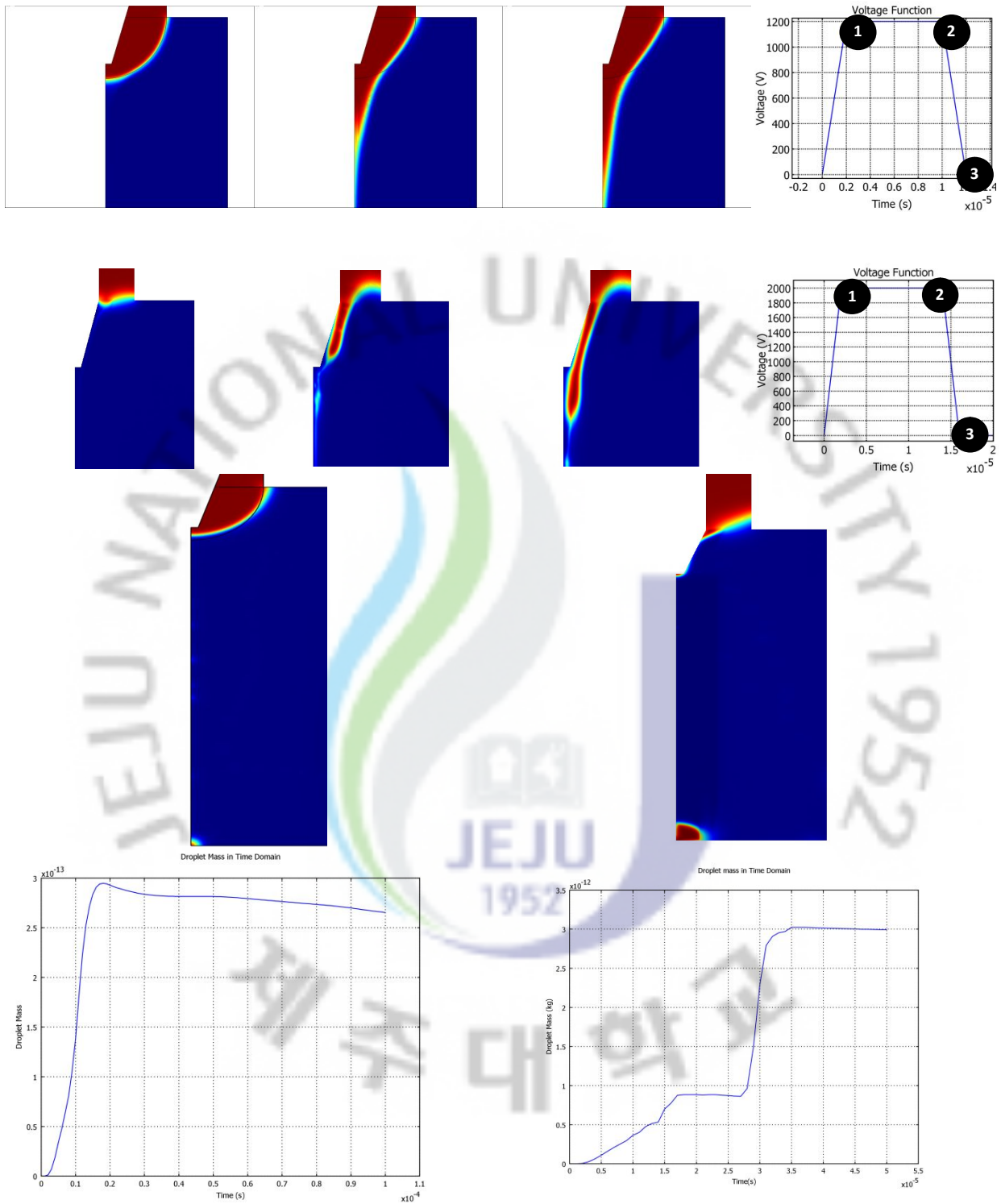


Figure 4.24. Comparison of Droplet Generation of Hybrid Electro-Piezoelectric and Electrostatic Inkjet

5 SUMMARY AND CONCLUSION

Even though electrostatic inkjet mechanism seems to be an attractive fabrication alternative for printed electronic devices but the application of electrostatic inkjet printing is hindered due to high viscous forces inside the microchannel of printhead assembly. Due to these forces the applied electrostatic potential for the ejection of the droplet is high and restrains the application of electrostatic printing for the commercial production of printed electronic devices. In the proposed work, two different type of methodology are suggested for partially overcoming the viscous forces present in the conventional electrostatic inkjet head.

The first approach used the electrokinetic pumping of microfluid for generating inertial stresses inside the microchannel. This method can supply the ink in precise manner and stable meniscus can be retained after the buildup of required meniscus before initiation of the electrostatic printing.

The second approach proposes a novel hybrid piezoelectric and electrostatic ejection process to be applied for the electrostatic inkjet head. The former approach is more suitable for the drop-on-demand process since the stable meniscus can be generated intermittently by means of piezo-actuation during electrostatic inkjet printing process.

5.1 CONCLUSION FOR CONSTANT FLOWRATE

The proposed electrokinetic pumping provides the insight of the importance of geometric shape and resulting fluidic channel flowrate. The first two cases for the increasing nozzle opening shows and tapered channel shows that the desired flowrate can be achieved through the primary horizontal channel discharging equal amount of flow to the secondary nozzle. Furthermore the manufacturing complexities of non-uniform outlet opening of the secondary nozzle can be overcome by electrokinetic pumping of the fluid stream from the primary channel.

In addition to above it also provides the possibility of modeling an electrokinetic intermittent pumping for the drop-on-demand inkjet application. Most of the work on drop-on-demand inkjet has been done by applying a constant flowrate with the help of syringe pump (Ishida et al.) [14] which has drawback of non-linear buildup of volume at the ejection meniscus during the low frequency drop-on-demand operation mode.

5.2 CONCLUSION FOR HYBRID PIEZO-ASSISTED

The simulation result of hybrid piezoelectric and electrostatic head shows that the size of the generated droplet in case of conventional electrostatic head is large and the electrostatic

ejection pulse required for the ejection of the droplet is long. Since the dynamic pressure needed to accelerate the liquid at rest inside the nozzle is high due to the viscous forces of the nozzle microchannel and the electrode itself. When the droplet is accelerated with the high electrostatic potential, the formed jet diameter is large and inertial forces are high. The combined effect of high electrostatic potential and inertial effect forms the droplet of bigger diameter than the one formed by the pre-developed meniscus.

Furthermore the simulation results also illustrate that the droplet ejection voltage can be reduced from 2kV to 1.2kV by generating the meniscus and applying the potential when the charging electrode becomes wet by the ink. Reduced voltage and smaller drop size for the droplet generation shows the significant improvement over the conventional electrostatic inkjet process.

Summary of the results for the hybrid piezoelectric and electrostatic head are as follows

- Reduced energy requirement by generating meniscus through piezoelectric actuation up to 40% (2kV to 1.2kV)
- Reduced the droplet size by more than 50%
- In case of simulation without meniscus the droplet size is around $18\mu\text{m}$ and meniscus formed by piezoelectric actuation the drop size is $8\mu\text{m}$
- Satellite drops for EHD simulation without meniscus
- Total time for the combined piezoelectric and electrostatic ejection is less than $100\mu\text{s}$
- Printing at 10kHz frequency is possible with the proposed hybrid printhead.

REFERENCES

- A. Castellanos (Ed.), "Electrohydrodynamics", CISM Courses and Lectures no. 380, Springer-Verlag, Wien, New York, 1998.
- A Kopf-Sill, "Commercializing Lab-on-a-Chip Technology," in *Proceedings of Micro Total Analysis Systems 2000*, Edition. A van den Berg et al. (Dordrecht, Netherlands: Kluwer Academic Publishers, 2000), 233.
- A. Berchtold, Lehrstuhl für Feingerätebau und Getriebelehre, Simulation of a drop-on-demand print head with planar piezoelectric transducer, IEEE, 1989.
- BH Weigl and P Yager, "Microfluidic Diffusion-Based Separation and Detection," *Science* 283 (1998): 346–347.
- Bruce R. Munson, Donald F. Young, Theodore H. Okiishi, "Fundamentals of Fluid Mechanics", John Wiley & Sons, 2002.
- C. D. Hendricks, R. S. Carson, J. J. Hogan, and J. M. Schneider, *AIAA J.* vol. 2, 733, 1964.
- D.A. Saville, "Electrohydrodynamics: the Taylor-Melcher leaky dielectric model," *Annual Review of Fluid Mechanics*, vol. 29, pp. 27 – 64, 1997.
- D. J. Beebe, G. A. Mensing, and G.M.Walker, *Ann. Rev. Biomed. Eng.* 4, 261 (2002).
- E. Cummings, S. Griffiths, R. Nilson, and P. Paul, "Conditions for similitude between the fluid velocity and the electric field in electroosmotic flow", *Anal. Chem.*, vol. 72, pp. 2526–2532
- Eric R.Lee, , 2003. "Microdrop GENERATION", *CRC Press*

- F. Mugele and J.C. Baret, "Electrowetting: from basics to applications", *Journal of Physics: Condensed Matter*, vol. 17, pp. R705–R774, 2005.
- Feynman R.P., Leighton R.B. and Sands M. 1964, *Addison-Wesley Publishing Company*, The Feynman Lectures on Physics
- Gravure Education Foundation and Gravure Association of America. *Gravure:Process and Technology*. Versailles, KY. 2003.
- H. A. Stone and S. Kim, *AIChE J.* **47**, 1250 (2001).
- H. Chen, Y.T. Zhang, I. Mezic, C.D. Meinhart, and L. Petzold, "Numerical simulation of an electroosmotic micromixer," *Proc Microfluidics 2003 (ASME IMECE)*, 2003.
- H. Morgan, N.G. Green, "AC Electrokinetics: Colloids and Nanoparticles", *Research Studies Press*, Hertfordshire, England, 2003.
- Hiroyuki Kawamoto, "Electronic Circuit Printing, 3D Printing and Film Formation Utilizing Electrostatic Inkjet Technology", *DF 2007, International Conference on Digital Fabrication Technologies*, Sept 16-21 2007.
- Hue P. Le, "Progress and Trends in Ink-jet Printing Technology", *Journal of Imaging Science and Technology* · Volume 42, Number 1, January/February 1998
- Hughes D C, Ernster S E 2003 Screen printed feature size capabilities. *Proc. IMAPS Conf. Exhibition on Ceramic Interconnect Technology: The Next Generation*, Denver, CO, USA, pp. 58–62
- J. Heinzl and C. H. Hertz: *Adv. Electron. Electron phys.* 65 (1985) 91.
- J.-U. Park, M. Hardy, S.J. Kang, K. Barton, K. Adair, D.K. Mukhopadhyay, C.Y. Lee, M.S. Strano, J.G. Georgiadis, P.M. Ferreira and J.A. Rogers, "High-Resolution Electrohydrodynamic Jet Printing," *Nature Materials* 6, 782-789 (2007)

- Kazuhiro Murata, "Super-fine ink-jet printing for nanotechnology", Proceedings of the International Conference on MEMS, Nano and Smart Systems (ICMENS'03), 346-349, 2003
- Kazuhiro Murata, J. Matsumoto, A. Tezuka, Y. Matsuba and H. Yokoyama, "Super-fine ink-jet printing -toward the minimal manufacturing system-", Proceedings of the Symposium on Design, Test, Integration Package of MEMS/MOEMS (DTIP'2004), 249-253, 2004
- Koo, H.-S. et al, "LCD-based color filter films fabricated by a pigment-based colorant photo resist inks and printing technology," *Thin Solid Films*, Vol. 515, (2006), pp. 896-901.
- LJ Kricka, "Miniaturization of Analytical Systems," *Clinical Chemistry* 44 (1998): 2008–2014.
- Mueller R, Gronmaier R, Janischowsky K, Khon E., "An all-diamond inkjet realized in sacrificial layer technology", *Diamond and Related Materials*, Vol. 14, 504–8, 2005
- NH Chiem and DJ Harrison, "Microchip Systems for Immunoassay: An Integrated Immunoreactor with Electrophoretic Separation for Serum Theophylline Determination," *Clinical Chemistry* 44 (1998): 591–598.
- P Yager et al., "Applying Microfluidic Chemical Analytical Systems to Imperfect Samples," in *Proceedings of Micro Total Analysis Systems '98*, ed. DJ Harrison and A van den Berg (Dordrecht, Netherlands: Kluwer Academic Publishers, 1998), 207–212.
- R. J. Melcher, "Continuum Electromechanics", MIT Press, Cambridge, 1981
- R. S. Carson and C. D. Hendricks, in AIAA Fourth Electric Propulsion Conf Paper No. 64-675, Aug. 1964.
- R. Elmqvist, Measuring instrument of the recording type, U.S. Patent 2566443 (1951).
- R. G. Sweet, High frequency recording with electrostatically deflected ink-jets, *Rev. Sci. Instrum.* **36**, 131 (1965).

- R. G. Sweet, Signal apparatus with fluid drop recorder, U.S. Patent 3596275 (1971).
- R. J. Pfeifer and C. D. Hendricks, *AIAA J.* vol. 6, 496, 1968.
- Satoshi Shigematsu, Yuji Ishida, Naotoshi Nakashima¹, and Tanemasa Asano, “Electrostatic Inkjet Printing of Carbon Nanotube for Cold Cathode Application”, *Jpn. J. Appl. Phys.* 47 (2008) pp. 5109-5112
- Sukhan Lee, Doyoung Byun, Sang Joon Han, Sang Uk Son, Yongjae Kim, Han Seo Ko, 2004. “Electrostatic Droplet Formation and Ejection of Colloid”, *Micro - Nanomechatronics and Human Science, 2004 and The Fourth Symposium Micro-Nanomechatronics for Information-Based Society.*
- Sukhan Lee Jeongtaek Oh Jihye Yang Doyoung Byun, “An Electrostatic Drop-On-Demand Micro Droplet Ejector with a Pole Type Nozzle”, *Nano/Micro Engineered and Molecular Systems, 2006. NEMS '06. 1st IEEE International Conference 18-21 Jan. 2006*
- T.M. Squires, M.Z. Bazant, “Induced-charge electro-osmosis”, *Journal of Fluid Mechanics*, vol. 509, pp. 217–252, 2004.
- Taylor, G. (1969) *Electrically Driven Jets. Proceedings of the Royal Society of London A: Mathematical, Physical & Engineering Sciences*, 313, 453-475
- W. E. DeShon and R. S. Carson, *J. Coll. and Interface Sci.* vol. 28, 161, 1968.
- W. L. Buehner, J. D. Hill, T. H. Williams, and J. W. Woods, *Application of ink-jet technology to a word processing output printer, IBM J. Res. Dev.* 21 (1968-1977).
- Wikipedia, http://en.wikipedia.org/wiki/Printed_electronics
- Wikipedia, http://en.wikipedia.org/wiki/Inkjet#Piezoelectric_inkjets

- Y.T. Zhang, H. Chen, I. Mezic, C.D. Meinhart, L. Petzold, and N.C. MacDonald, "SOI Processing of a Ring Electrokinetic Chaotic Micromixer," Proc NSTI Nanotechnology Conference and Trade Show (Nanotech 2004), vol. 1, pp. 292–295, 2004.
- Yin, X. and S. Kumar. 2005. "Flow visualization of the liquid-emptying process in scaled-up gravure grooves and cells." *Chemical Engineering Science*, 61:4:1146-1156.
- Youngmin Kim, Sanguk Son, Jaeyong Choi, Doyoung Byun, and Sukhan Lee, "Design and Fabrication of Electrostatic Inkjet Head using Silicon Micromachining Technology", *Journal of Semiconductor Technology and Science*, Vol.8, No.2, June, 2008
- Yuji Ishida, Keigo Sogabe, Shintaro Kai, and Tanemasa Asano, "Droplet Ejection Behavior in Electrostatic Inkjet Driving", *Japanese Journal of Applied Physics*, Vol. 47, No. 6, 2008, pp. 5281–5286.

